ELECTROCHEMICAL ENERGY SOURCES

Bruno Mazza
Dipartimento di Chimica Fisica Applicata
Politecnico di Milano
Via Mancinelli 7, I20131 Milano

COMETT
Community Programme for
Education and Training in Technology

Course
"New Trends in Industrial Electrochemistry"
Palermo, November 7-10, 1994

For non-specialists' use and convenience, a list of definitions of the most common electrochemical terms concerning electrochemical energy sources has been taken from Reference 7.
The topics discussed in this lecture, as well as in the following one, can be framed into a clear chronological table of the developments of electrochemistry which has been taken from Reference 13.

1. Secondary Batteries (4,7)

A summary of the most desirable characteristics for cell reactants and electrolytes is given in Slide 1.
Some perspective regarding the relative specific energies of various electrochemical cells can be gained by studying Slide 2, which shows the theoretical specific energy of various cells plotted versus the equivalent weights of the reactants. The theoretical specific energy is defined as the Gibbs free energy change for the overall cell reaction, divided by the corresponding weights of the reactants: $-\Delta G/\Sigma\nu_r M_r = nFE/\Sigma\nu_r M_r$, where ν_r is the number of moles of reactant r, M_r is the molecular weight of reactant r, n is the number of the electrochemical equivalents involved in the cell reaction, and E is the emf of the cell reaction. It is evident from Slide 2 that higher theoretical specific energy values correspond to cells with low - equivalent - weight reactants, and with large electronegativity differences between the reactants. The alkali metals are very attractive reactants for the negative electrodes, and the chalcogens and halogens (and some compounds containing them) are very attractive reactants for the positive electrodes. Please note that most of the high-specific energy couples involve reactants that are incompatible with aqueous electrolytes.

How does one use the figure in Slide 2 in assessing the specific energy that might be obtained from a cell of practical design and construction? The following is a reliable set of guidelines: multiply the theoretical specific energy by 0.2-0.25 for cells with solid reactants, and by 0.15 for cells with an air electrode. These multipliers apply for systems developed to provide reasonable cycle life, at a minimum weight.

The theoretical specific energy of the lead acid battery can be estimated starting with the overall reaction equation:

$$Pb + PbO_2 + 2\ H_2SO_4 \underset{\text{charge}}{\overset{\text{discharge}}{\rightleftarrows}} 2\ PbSO_4 + 2\ H_2O.$$

The weights of the species involved amount to 642.4 g, while the exchanged electric charge is 2F = 53.61 Ah. Using the standard emf 1.930 V, the theoretical specific energy is: (53.61)(1.930)/0.6424 = 161 Wh/kg. In practice only one quarter of this can be attained. To explain this great difference between theory and practice the proportionate weights of the different construction elements are compiled in the upper figure of Slide 3. The scale on the left shows the weights which are needed per kWh, while the reciprocal numbers (Wh/kg) are plotted on the right.

The bottom block in this figure contains the overall reaction equation, which leads to the above calculated value of 161 Wh/kg, which means that a weight of 6 kg would be able to store 1 kWh. However, pure H_2SO_4 is not an electrolyte; the acid has to be diluted to achieve adequate conductivity. Furthermore there must be some acid excess to keep conductivity even when the battery becomes discharged completely. Therefore the pure electrochemical system provided with the correct acid requires 11.5 kg/kWh. Additional weight is caused by the fact that only a fraction of the active material can be utilized. At extremely low discharge rates mass utilization may be increased to about

70%, but at ordinary rates (in the order of magnitude of hours), this figure drops to about 35%, reducing the available specific energy to nearly 50 Wh/kg. The limited mass utilization can be explained bearing in mind that chemical reactions occur at the electrode. During discharge, e.g., lead is dissolved at the negative electrode and lead sulfate precipitated, while at the positive electrode PbO_2 is reduced and dissolved Pb^{2+} ions give rise to lead sulfate precipitation. These reactions produce isolating layers on the active material which prevent further discharge. Furthermore dismantling of charged material by dishomogeneous attack will reduce the electric contact between parts of the active material and the grid, also restricting further discharge. In addition to the facts discussed so far, much extra weight is added by passive construction elements which are unavoidable in the actual lead-acid cell. So the grids supporting the active material and conducting the current usually contribute for nearly as much weight as the active material itself does. But the acidic environment and corrosive potentials exclude the substitution by lightweight metals. The same is true for the so-called top lead, i.e. the conducting bars at the top of the plates and terminals. Finally, the cell has to have a jar which (as well as the isolating separators between the plates) does increase the weight. Therefore, in pratice, even cells for electric vehicles, which are developed especially for low weight, deliver less than 40 Wh/kg and little margin is left for further increase.

The lower figure in Slide 3 shows the weight analysis of a typical starter battery (SLI stands for starting, lighting, ignition).

Grid design (Slide 4) is meant to suit a number of parameters (e.g. weight, corrosion resistance, strength, and current distribution) which are important in different ways for

different battery applications. Since the melting point of lead is low (327 °C), most grids are formed by melting and casting; some lighter varieties are now manufactured using a stretching process (see in Slide 5 a process developed by Magneti Marelli) which produces expanded metal perforated sheets. Grids are designed to ensure a low internal resistance for the cell and to minimize shedding of active material on cycling. Shedding causes loss of capacity, and dislodged material can accumulate on the battery case floor where it can give rise to short circuits between positive and negative plates. Small additions of tin are made to the lead to improve its coating properties, while antimony, calcium or selenium are added to form alloys with better stress resistance. Lead-antimony was the first alloy used and still remains the most popular one. Antimony (1.5-8%) greatly improves the mechanical properties of grids and connector bars, but it also increases their electrical resistance, accelerates the self-discharge of the cell, and reduces cycle efficiency. Lead-calcium grids (manufactured using the new process shown in Slide 5) exhibit superior performance in many ways.

The main component of the paste used to fill the grid is known as lead dust, and consists of a carefully milled mixture of metallic lead and lead oxides. Water and sulfuric acid are added in predetermined sequence, together with minor components and strengthening fibres, and the resulting slurry is loaded onto the grids and "cured" or dried to produce a crack-free plate, with good adherence to the grid. The active material is later converted to the fully charged condition by the forming process.

Plates are assembled into parallel groups or stacks (usually with one extra negative plate), which are then interleaved, with separators, retainers and spacers inserted (Slide 4). In a battery containing more than one cell group series

connections must also be made. In modern SLI batteries such connections are made within the battery case using through-partition ties, thus saving lead and reducing the internal resistance and weight of the battery (Slide 4).
In Slide 6 the assembly of the type of cell used in a traction battery is shown: the multi-tubular positive plates give the cell high specific energy and capacity and assure a long cycle life. Tubular plates (also known as "armoured" or "clad" plates) consist of a row of tubes containing axial lead rods surrounded by active material. The tubes (which generally have a circular cross-section) are made of fabrics such as terylene or glass fibre or of perforated synthetic insulators which are permeable to the electrolyte. Tubular plates are strong enough to withstand continuous vibration and are resistant to shedding. They are also able to sustain many deep discharges without loss of integrity.
A new generation of lead acid batteries characterized by a sealed configuration is being developed, i.e. the valve regulated lead acid (VRLA) batteries. They are spill-proof as the acid is immobilized either by gelling or by absorption into a microporous glass fibre separator. The recombination technology eliminates the danger of excessive hydrogen evolution and the need for water additions. Therefore, this type of lead acid battery presents very interesting properties, such as emission- and maintenance-free and easier installation without dedicated housing.
Slide 7 (left) illustrates a cell configuration proposed for the sodium-sulfur battery (a new type of battery technology at the pre-series status). The cell operates at a temperature > 300°C where both the metallic-sodium anode and the sodium polysulfide Na_xS of the cathode (which is formed during discharge) are molten. A molten Na_xS is capable of accepting a large concentration of sodium and diffusion into the melt is rapid enough. The solid electrolyte is a Na^+-ion conductor

(beta-alumina; see Slide 7, right), and extraction of the Na^+ ions as Na into the Na_xS cathode, which is also an electronic insulator, requires the supply of electrons from a carbon felt attached to a corrosion-resistant metal rod. A completed cell should, of course, be sealed with a cap material matching the thermal expansion of the solid electrolyte. In operation, temperature cycling through the melting temperatures of the electrodes should not break the seals or crack the large-area, thin electrolytes.

Special attention has also been given to the zinc-air battery. A number of attempts to build a sample device by coupling a zinc electrode with a fuel cell air electrode (see below) have been made, but the problems of the air electrode (considerable polarization losses) are combined to those of recharging the zinc electrode (concerning the morphology and distribution of electrodeposited zinc). Another serious problem is the carbonation of the alkaline electrolyte. In some cases, the replacement of the zinc electrode has been practiced as a means of "mechanically" recharging the battery. The advantages of this are that the zinc electrode is not recharged in-situ, and thus does not suffer from dentrite formation, shape change (zinc redistribution), etc. In addition, the air electrode is not required to operate as an anode, thus providing for a greatly extended life (operation during recharge tends to cause damage to the air electrode structures and electrocatalysts, rendering them less active for oxygen reduction). This system is being developed, among others, by Edison Termoelettrica (Slide 8).

Some candidate energy sources for electric vehicles are shown in Slide 9. In reviewing the status of the individual candidate systems, it becomes clear that meeting the performance, durability, and cost goals simultaneously represents a difficult but very important challenge. Each system reviewed has its own strong points and deficiencies.

2. Power and Energy Requirements for Electric Vehicles (4,5)

In order to devise appropriate batteries for electric vehicles, it is necessary to know the power and energy requirements of the vehicle. These can be computed in a straightforward manner from the equations of motion of the vehicle, and typical driving profiles (velocity vs. time).
The equations of motion are reported in Slide 10.
Several driving profiles are presented in Slide 11 on the left. These were used in conjunction with the equations above to yield the power profiles shown in Slide 11 on the right, for a vehicle mass of about 1700 kg. It has been found that the energy consumption per unit distance, per unit vehicle mass is not very sensitive to the details of the driving profile, so that the results of the many computations can be summarized in the simple form of Slide 12. A convenient set of numbers for battery design use is an energy consumption of 0.15 kWh/T km, or 0.15 Wh/kg km, and a power of 35 kW/T for acceleration (still referring to unit vehicle mass).
For a good vehicle design, a maximum of 30% of the vehicle mass may be assigned to the battery. This allows an estimate of the vehicle range to be made, if the specific energy of the battery is known. Conversely, for a desired vehicle range, the required specific energy of the battery can be calculated (Slide 13). For a vehicle range of 150 km, and $f_b = 0.3$, the specific energy of the battery must be 75 Wh/kg. Any battery with a lower specific energy cannot achieve a 150 km range in a well-designed electric vehicle. This is the major problem for battery development.
As a conclusion, when the performance and range needs for electric automobiles are taken into consideration, it is clear that a power source capable of providing more than 100 W/kg acceleration power, and more than 70 Wh/kg energy storage capability is necessary if a range of 150 km is to be

achieved.

A simple but useful reflection of the relationship between the specific energy (Wh/kg) and the specific power (W/kg) of various batteries is shown in Slides 14,15, and 16. The lines curve toward lower specific energies at higher specific powers for a number of reasons, including higher voltage losses (resistive and other) at higher power levels and lower active material utilizations at higher power levels. Design improvements to make these curves more nearly vertical usually add weight, and cause the low specific power ends of the curves to shift to the left.

The specific power required for reasonable acceleration is shown as 120 W/kg in Slide 14. All candidate batteries must have this capability for 10-20 s for each major acceleration, over most of the capacity of the battery (0 to 75-80% depth of discharge) and over most of its range of operating temperatures.

In the figures shown in Slides 15 and 16 an overlaid grid marks the projected range an electric automobile of a given weight could travel at certain speeds. For example the upper figure in Slide 16 shows that a commercially available lead-acid battery has a capacity of 40 Wh/kg at the 2 W/kg level (corresponding to the 20 hours discharge rate) but indicates a drop to 10 Wh/kg when the power demand rises to about 40 W/kg. At the same time, this means that a car travelling at 80 km/h would only have a range of 20 km, very marginal, thus reflecting the real situation of todays electric automobile technology, not counting battery and car improvements which are only in the research and early development stage. Of course, for the moderate requirements of fleet vehicles (postal vans, delivery trucks) not exceeding 50 km/h the range becomes 80 km, which is definitely useful in the city, relieving environmental problems.

Variation of specific power with specific energy for fuel

cells (see Slides 15 and 16) shows the similarity of fuel cells (see below) to a heat engine rather than a battery. In batteries, at least one of the reactants is stored within each cell, and the specific energy of the system tends to be a performance-limiting factor. In fuel cells, neither reactant (fuel or oxygen from air) is stored in the cell, and the specific power of the system tends to be a performance-limiting factor. Hence, it appears necessary to hybridize a fuel cell with a battery for vehicular applications.

Slides 17 and 18 show the performance characteristics of a passenger automobile, a postal service vehicle and a commercial van developed as a demonstration of technology. For comparison's sake, the performance characteristics of an internal-combustion engine automobile are listed in Slide 19. As far as environmental and energy utilization issues are concerned, the electric vehicle must be considered as a total system which includes the primary energy source, electric power generating plant, and the distribution network of electrical power, as shown in the upper figure in Slide 20. In comparison, the combustion engine vehicle must also be considered as a total system which includes the primary energy source, a chemical fuel processing plant, and a fuel distribution network, as shown in the lower figure in Slide 20. These two vehicle systems are very similar in many aspects but also have a very distinct and important difference. Both systems include a Carnot-limited energy conversion step which is the efficiency-limiting step in the total process and is also the step in the process where there is direct interaction with the air and/or water environment. In the case of the electric vehicle system, this conversion step is carried out in a relatively small number of large stationary equipment installations as contrasted to being carried out at the point of vehicle usage in million of small, mobile combustion engines. Although this might appear

to be a rather subtile difference, it is a particularly important aspect of the environmental issues related to electric vehicles.

A significant expression of the interest of the electric boat for assuring the environment friendly mobility on water is the initiative of the development of an electric water-bus for public service in Venice, or an "electric vaporetto". The initiative started in 1989 and was based on a cooperation between ACTV (the Public Transport Authority of Venice), CETENA (the Centro Studi Tecnica Navale), ENEL (for energy supply and technical support), Alutecna (for the development of the frame in light weight alloy), Ansaldo (for the electric propulsion system), and Magneti Marelli (for the battery). The "electric vaporetto", after a long trial is presently in service. The appreciated achievements are the absence of emission, the reduction of noise and vibrations, with the consequence of passenger comfort, and the reduction of waves, which can damage the structures. The main characteristics and the layout of the water-bus are shown in Slide 21. The daily service of the electric water-bus is performed by making use of the battery interim recharging. Slide 22 shows the resulting state of charge of the battery during the daily mission. This procedure, beside the direct effect of extending the range according to the mission requirements, is also beneficial for the battery life, insofar it avoids deep discharge. In a new demonstration programme the "electric vaporetto" should be hybridized with a Diesel engine.

3. Fuel Cells (4,5)

A typical fuel cell power plant consists of three units (Slide 23): fuel processor (or conditioner), fuel cell, and power conditioner. These units are essentially modular in nature and can be connected in parallel or in series to meet additional power demands.

Fuel cell power-generation systems, grouped into four distinct classes differentiated by the electrolyte used in the fuel cells, are (1) acid type, including phosphoric acid (first generation), sulfuric acid, and solid polymer electrolyte; (2) alkaline type; (3) molten carbonate type (second generation); and (4) solid electrolyte type (third generation). (See Slide 24).

Hydrogen-oxygen fuel cells employ porous gas diffusion electrodes (Slide 25), which constitute the essential components of such electrochemical energy conversion devices (by such electrodes, not only activation overpotential but also concentration overpotential is decreased significantly). As a matter of fact, gases have very low solubility in electrolytes. Consequently, to achieve practical current densities (at least 200 mA/cm^2), it has been necessary to use porous electrodes with the gas supplied through the porous structures to the electrode-electrolyte interfaces within the porous structures. Thus, porous electrodes feature the complexities of three-phase systems with solid, liquid, and gas partecipating in the electrochemical reaction. In this triple-contact area, the maximum exchange among the gas, the electrode and the electrolyte is achieved (Slide 26).

In order to immobilize the liquid meniscus within the porous electrode, two types of approaches have been used: (1) completely hydrophilic porous electrode in which the contact angles promote wetting; and (2) semi-hydrophobic porous structures with part of the electrode pore structure having

non-wetting internal surfaces (see Slide 27).
The hydrophilic electrodes have usually been constructed with sintered metal particles such as silver. Such electrodes have a fine pore layer on the side of the electrode towards the bulk electrolyte and a coarse pore layer on the rear gas side. A sufficient excess of gas pressure is maintained on the rear side to maintain the electrolyte meniscus in the transition region between the fine and coarse pore layers and yet not to blow gas into the electrolyte. This requires very close control of the pore size distribution in the manufacture of the electrodes.
The semi-hydrophobic type electrodes rely on contact angles greater than 90° rather than excess gas pressure to maintain the meniscus in a stable configuration within the porous electrodes. A thin highly hydrophobic (water repellent) layer prepared using Teflon or a Teflon-carbon mixture is often utilized as an air permeable porous backing layer through which electrolyte could not normally penetrate. On the electrolyte side is a wetted very high area layer containing the catalysts normally consisting of carbon plus an additional catalyst such as platinum or silver.
Slides 28 and 29 show the cell structure, stack structure, electrode structure, and catalyst structure of a phosphoric acid fuel cell, with particular reference, in Slide 29, to a Fuji Electric 50 kW demonstration package unit for on-site applications, installed at Eniricerche near Milan on behalf of Snam and ENI. The fuel cell stack is constituted by cells (consisting of an anode, cathode, and a matrix for holding the phosphoric acid electrolyte, see below) and separators for separating the reaction gas placed between the cells and cooling plates at each multiple cells. The fuel cell stack also has clamping plates to apply the necessary compression stress to the current collectors, electric insulating plate, and cells. The manifolds are placed around the fuel cell

stack.

At the air electrode, the electrochemical reaction of the cell is: $\frac{1}{2}\ O_2 + 2H^+ + 2e^- = H_2O$. The oxygen in the air which flows through the gas channels of the electrode substrate passes through the gas diffusion part of the electrode and is diffused to the electrode catalyst layer. The electrode catalyst layer is constructed by dispersing the catalyst agglomerate which is platinum or platinum alloy supported on carbon black and polytetrafluoroethylene bonder. Phosphoric acid is also maintained at the catalyst agglomerate so that the hydrogen ions migrate. The diffused oxygen is dissolved and transported to the platinum surface by the catalyst agglomerate surface phosphoric acid. Thereupon, the hydrogen ions and oxygen in the phosphoric acid react with the electrons propagated through the electrode substrate and carbon black and water is generated. The generated water is fled to the electrode substrate gas channels and is carried to the outside of the cell over a reversed path of the oxygen path. The air electrode reaction ($\frac{1}{2}\ O_2 + 2H^+ + 2e^- = H_2O$) and fuel electrode reaction ($H_2 = 2H^+ + 2e^-$) are performed via an ion conductive electrolyte and power is generated by flowing electrons through an outside circuit.

Slide 30 shows the block diagram of a phosphoric acid fuel cell power plant, with particular reference to the 1 MW demonstration unit for dispersed generation built in Milan by Ansaldo, based on a cooperation with AEM (the Milan Municipal Energy Authority) and ENEA; the plant uses fuel cell stacks supplied by IFC (International Fuel Cell) and a methane reforming system supplied by Haldor Topsoe. (The experience gained by Ansaldo in designing and constructing the plant and the results that will be obtained by AEM, the company which now owns the plant, during its operation, are essential to prepare for the introduction of fuel cell plants into the Italian electric system).

The major functional components of the plant are the fuel and air processing subsystems, a fuel cell power section, and a thermal management subsystem. Air is compressed in a turbocompressor before being fed to the cathode. The reformer-burner effluent provides the energy to drive the turbine of the turbocompressor unit. Methane also is compressed and then passes through a hydrotreater (hydrodesulfurizer), where sulfur compounds are removed. The clean fuel is then mixed with steam from the power section waste heat. The fuel-steam mixture passes into the heat exchange reformer where it is processed to a mixture of hydrogen, carbon dioxide, carbon monoxide, and water vapor. The carbon monoxide and the water are then further converted to hydrogen and carbon dioxide in two shift converters operating successively at lower temperatures. The low-temperature shift converter reduces the carbon monoxide concentration to less than 1% (carbon monoxide and sulfur impurities are deadly poisons for hydrogen electrodes). The processed fuel then flows to the anode cavities in the fuel cell power section, where hydrogen is extracted for the electrochemical reaction. The anode exhaust stream then enters the reformer burner, where the dilute hydrogen is burned to provide heat for the reforming process.

Basic specifications of both the Fuji 50 kW package unit installed at Eniricerche near Milan, and the ICF 1 MW plant installed at AEM inside the Milan urban area (Bicocca) are listed in Slide 31.

Alkaline fuel cells offer higher performance than phosphoric acid fuel cells. The cell voltage (0.8 V) is higher than that (0.7 V) of the acid cell because of the observed lower cathodic overpotentials in the alkaline cell. The cathodes do not require noble metals, which results in a substantial cost reduction when compared to the acid cells. A further advantage of alkaline cells is that nickel, which is stable

in the cell environment, can be used for fabrication of electronically conductive components (e.g. electrodes, current collectors). In contrast, acid systems are restricted to expensive materials, such as graphite, tantalum, or niobium. Carbon dioxide, in air or in fuel gas, fed to the cell causes a rapid carbonation of the electrolyte and loss of performance. Consequently, a carbon dioxide scrubber is necessary, prior to the cell inlet, to prevent this problem. At present, the energy required for carbon dioxide removal is rather high and, hence, the efficiency advantage of the alkaline fuel cell, resulting from lower cathodic polarization, is almost totally negated by the efficiency penality associated with elimination of carbon dioxide from the air and fuel gas streams. If the carbonation problem can be overcome without significantly increasing capital costs and reducing overall efficiency, alkaline fuel cells will be attractive for large-scale power generation.

Slide 32 shows the cell structure of a molten carbonate fuel cell, which employs a mixture of alkali metal carbonates in a ceramic particulate matrix as the electrolyte and porous nickel based electrodes as anodes and cathodes. The molten carbonate fuel cell power plant has several significant advantages over a system using acid cells because of the higher power density at higher voltages than with the acid cell. The fuel processor is simpler since the cell is tolerant to carbon monoxide and the reforming process can occur within the fuel cell. As a result, reformer and shift converter are not required. Higher efficiency is achieved because the reforming process absorbs heat, which would be supplied in situ by heat produced at the electrodes of the cell. Furthermore, the cell operation at high temperature (600-750°C) is conducive to the use of process air for cooling (lower temperature acid cells require a separate coolant loop). In large systems, it is anticipated that

increased efficiency can result by recovering waste heat in order to generate steam for use in a steam turbine or as process steam.

Slide 33 shows the sketch of a solid electrolyte fuel cell, which is essentially a hydrogen-oxygen fuel cell with a solid, ceramic oxide material serving as the electrolyte, the mechanism of ionic conduction being oxygen ion transport via anion defects in the solid oxide crystal lattice. High-temperature (~ 1000 °C) solid electrolyte fuel cells have many advantages over other types of fuel cells as there are no liquids involved and, hence, the problems associated with pore flooding and maintenance of a stable three-phase interface are totally avoided. In addition, the electrolyte composition is unvaried, regardless of the composition of the fuel and oxidant streams, and activation polarization losses are negligible. Fuel power plants using solid electrolyte cells are designed to have a high overall system efficiency through integration with a fuel processing system. As with the molten carbonate fuel cells, the cell is compatible with carbon monoxide, and the reforming process can take place in the cell; the fuel processing system for a solid electrolyte cell is thus simplified relative to the requirements for an acid cell system. Carbon dioxide is not required as a cathode reactant and, therefore, the solid electrolyte cell offers a somewhat simpler power plant system than the molten carbonate cell. Also, the higher operating temperature facilitates waste heat rejection and integration with other power plant functions. Furthermore, the solid electrolyte cell power plant has a unique advantage when coal is employed as a fuel in that the waste heat generated can be employed to gasify coal, thus providing fuel gas for the fuel cells. Thermal coupling leads to high overall efficiencies for the power system and, practical efficiencies of more than 60% are considered much likely. This efficiency is significant, as

this type of power system utilizes coal rather than natural gas, methanol, or naphta as fuel.

As far as the solid polymer electrolyte (i.e. a quasi-solid electrolyte) fuel cells are concerned, Slides 34 and 35 describe the Gemini spacecraft fuel cell system, which successfully met in 1965 the requirements of manned 7- and 14- day missions (please remind that ion-exchange membrane fuel cells were unknown in 1954). The membrane was a polystyrene divinyl benzene sulfonic acid type membrane, denoted by P(S-DVB)SA. Afterwards, perfluorinated sulfonic acid membranes were developed, with a greatly enhanced chemical stability to strongly oxidizing environments due to the absence of any hydrocarbon linkage in the backbone. The electrodes were directly applied on both sides of the membrane. The advantage of such a system over the traditional one, based on porous, gas-permeable electrodes detached from a porous separator, is evident, since by the new method one sets aside the delicate problem of metering the gas feed through special porous electrodic structures in such a way as to prevent any loss of unreacted gas into the electrolyte or the flooding of the electrode pores. The membrane itself operates as a solid electrolyte, hence the trade name of SPE (solid polymer electrolyte).

Recent progress in solid polymer fuel cells makes this technology very attractive for transportation applications, via methanol reforming, and using a hybrid system with a secondary battery. Such a hybridized system would be characterized by fuel cell and reformer tailored to generate an "average" power and operating under nearly stationary conditions, and by high cycle number long-life batteries sized to meet the power peaks and warm-up requirements (cold start-up). (In this way the fuel cell-reformer system may exhibit a less extreme dynamic behavior and be subject to slow variations of operating conditions). In order to develop

cell and stack technology a cooperation was established in 1989 between ENEA and De Nora Permelec. De Nora cells with Du Pont (Nafion) and Dow membranes have been built and tested with very promising results (more than 20 small scale (< 1 kW) units operated during the last year for an overall amount of about 1000 hours; six months of intermittent operation successfully tested; 1 kW unit tested c/o Ansaldo facilities under extreme conditions; six months on the shelf life verified). Stacks design and construction is continuing, the goal being a 10 kW stack (a 5 kW not optimized unit, based on a cheap, mass producible hardware design was completed by the end of 1993 and is presently being tested at Ansaldo facilities; 9 units will be delivered to the EQHHPP bus project for a total amount of 45 kW at the endplates and other 9 units will be delivered to the EQHHPP boat project). (See Slides 36 and 37). Within the frame of the Euro-Quebec Hydro-Hydrogen Pilot Project (EQHHPP, 100 MW of hydropower made available in Canada to produce hydrogen by electrolysis, which will then be shipped to Europe in the form of liquid hydrogen for use in the transportation and energy intensive industry fields), a city bus with electric drive and battery storage will be powered by a membrane fuel cell system (from De Nora) with liquid hydrogen as fuel in superinsulated tanks mounted on board, and a small (approx. 20 m long) public transport boat on the Maggiore Lake will be converted to membrane fuel cell propulsion (De Nora) and liquid hydrogen storage (Italian partners: Ansaldo, ASM Azienda Servizi Municipalizzati Brescia, GNL Gestione Governativa Navigazione Laghi Maggiore-Garda-Como, ISTIC Università degli Studi di Genova, RINA Registro Italiano Navale, SERE Servizi e Ricerche Elettrochimiche De Nora).

ENERGY RECOVERY IN ELECTROCHEMICAL CELLS

Bruno Mazza
Dipartimento di Chimica Fisica Applicata
Politecnico di Milano
Via Mancinelli 7, I20131 Milano

COMETT
Community Programme for
Education and Training in Technology

Course
"New Trends in Industrial Electrochemistry"
Palermo, November 7-10, 1994

4. Energy Recovery from an Amalgam Denuder (2,10)

As it is well known, the comparison between the amalgam process and the diaphragm (or membrane) process for making chlorine and caustic indicates a difference of the decomposition (reversible) voltages by about 1 V. Caustic soda is produced directly by the diaphragm cell; on the other hand, in the amalgam process, sodium amalgam formed at the amalgam cathode must be decomposed in a separate cell, named the amalgam decomposer (or denuder), to convert into caustic soda. Amalgam decomposition is an electrochemical process, but exothermic, and hence it takes place without an external power supply. That is, the sodium amalgam anode and the hydrogen cathode on graphite lumps in the decomposer form a short-circuited local cell. The overall process consisting of the amalgam formation reaction (electrolysis) and the amalgam decomposition reaction is, of course, equal to that of the diaphragm cell. Therefore, the decomposition voltage of the amalgam cell system will become equal to that of the diaphragm cell if the free energy change for amalgam decomposition is recovered as dc electric power by an adequate procedure such as fuel cell technology.

Slides 38 and 39 give an idea on this concept, where the electric energy equivalent to about 1 V could be recovered by the amalgam decomposition fuel cell connected with the amalgam cell. Practically much lower voltage savings may be obtained because the hydrogen overpotential of the cathodic reaction on the commercial available electrocatalysts in the presence of concentrated caustic is very high, even at current densities lower than those used in mercury cells. The system shown has another serious problem. The current efficiency of the amalgam cell is 92-95%. Therefore, the anodic oxidation of mercury may take place due to unbalance of 4-8% of current efficiency in the amalgam decomposition

cell. Separate circuits to balance the reactions will increase investment cost.

Slide 40 illustrates the original Castner rocking cell. It comprised three sections, two outer brine cell compartments with graphite anodes and a central amalgam denudation compartment. The sodium amalgam formed in one brine compartment was transferred to the denuder and then on to the second brine compartment by imparting a periodic rocking motion to the cell so that only one of the brine compartments was operational at a time. The amalgam also served to provide separation of the three compartments. Attempts were made to recover energy from the denuder, but considerable work showed this to be impracticable at industrial scale (see above). So the denuder changed into a short-circuited cell in which the iron grid was connected to the amalgam.

In principle, the air cathode (see below) can also be used to recover electrical energy in conjunction with mercury cells through the use of an electrochemical amalgam denuder (Slide 41). In fact, if the oxygen reduction cathode is applied in the amalgam decomposition cell instead of the hydrogen evolution cathode, a large emf, say 2.2-2.4 V, can be obtained. Unfortunately, the high irreversibility of the cathodic oxygen reaction even on the most suitable available materials and at current densities far below those of the electrolytic cells, prevents the practical application of such technology too. A high performance fuel cell of the form $Na(Hg)/NaOH/O_2$ was built in the early 1960's in the United States for military application. To make such an electrical energy recovery system practical for the chlor-alkali application involves many difficulties and high capital expenditure. Furthermore, new mercury cell construction is unlikely because of environmental problems: the better approach is not to generate amalgam in the first place.

As a conclusion, all attempts to recover energy from an amalgam denuder have failed.

5. Chlor-Alkali Electrolysis with Oxygen Depolarized Cathodes (5)

The hydrogen generated in present diaphragm and membrane chlor-alkali cells is usually burned for its heat value rather than used for chemical purposes. In such instance the replacement of the hydrogen generating cathodes with air consuming oxygen cathodes offers the opportunity for substantial energy savings (Slides 42,43,44). This variant suggested itself when, on the one hand, gas-diffusion cathodes improved by the fuel cell technology could to a sufficient extent be made available at least for pilot plant operations, and on the other hand, the membrane cell process was capable of supplying a pure caustic soda solution separated from the anolyte (a high purity catholyte is much less likely to present poisoning problems with respect to air cathode catalysts). According to the thermodynamic decomposition voltages, it would in this way be possible to save at best 1.23 V of usual membrane cell voltage. In practice, even in comparison with highly catalyzed hydrogen cathode, the air cathode is still expected to ensure a voltage saving of 1.0 V (~ 28%, but the total energy saving will be less since the heat value of the hydrogen will no longer be available).

In Slide 45 the oxygen cathode structures of both the hydrophilic type and the semi-hydrophobic type are shown (see the discussion on the porous gas diffusion electrodes in the previous lecture). For in - situ chlor - alkali applications the hydrophilic type oxygen cathodes appear less attractive than the semi-hydrophobic type. Sintered metal electrodes tend to be considerably more expensive to fabricate particularly when the pore size distribution must be carefully controlled and it is difficult to make them very thin without structural support-cracking problems. As to the

semi-hydrophobic electrode structure, note in Slide 45 the gas-filled capillaries or wicks made up of Teflon particles in chain like clusters of fibrils which extend into and through the active layer and expedite transport of the oxygen into the whole active layer.

Despite the attractiveness of in-situ air cathodes for chlor -alkali cells, there are still significant problems such as the sluggishness of the oxygen electrode (the relatively high cost of ion selective membranes leads to high current density requirements, because of capital investment considerations, for example 300 mA/cm^2, which is a rather high current density for oxygen electrodes), the electrode cost (relatively high, particularly if platinum is used as the catalyst at substantial loadings), and the operational life (which should be a minimum of one year with very low failure statistics at shorter times). Moreover, it is necessary to remove nearly all of the carbon dioxide from the air supply to prevent carbonate precipitation within the electrode active layer.

An alternative to the in-situ air cathode is to use hydrogen in hydrogen-air fuel cells such as the first generation phosphoric acid system. These cells operate at temperatures up to 200 °C and the cogenerated heat would be available for concentrating the caustic particularly with diaphragm chlor-alkali cells. Further, unprocessed air can be used because of the carbon dioxide tolerance of the acid fuel cell systems. A major advantage is that these cells could be retro-fitted to existing diaphragm chlor-alkali cells. Another advantage of the hydrogen-air fuel cell approach (utilizing by-product hydrogen from chlor-alkali cells) is that the hardware is largely available. The operating voltage, however, is presently ~ 0.6 V and hence the recovered electric power is only ~ 60% of that with the in-situ air cathodes.

6. Electrolysis with Hydrogen Depolarized Anodes (12,32,36)

As well known, the industrial production of caustic soda is today linked to the co-production of chlorine gas in a ratio of about 0.9 ton of chlorine for each ton of caustic soda. The technologies today available are (1) mercury, (2) diaphragm, and (3) membrane, with a specific consumption of electric energy of about 3000, 2500, and 2200-2500 kWh/T caustic soda respectively. Chlorine demand has been decreasing in the last few years due to the market difficulties which have particularly affected the chlorinated solvents and the pulp and paper industries, whilst caustic demand is steadily increasing. In the meantime many industries have to face the continuously worsening problems related to the disposal of large quantities of salts, mainly sodium salts as by-product from chlorine dioxide plants, pulp and paper industries, rayon plants, acid waste neutralization from different chemical processes and pharmaceutical industries. These salts, up to recent times, were disposed of by dilution in the bulk of effluents or dumped into disposal areas or, in the specific case of sodium sulfate, utilized by the solid detergent and glass industries as an inert charge in their formulations. Their disposal/utilization possibilities are going to decrease or to disappear in the very near future due to the possible shortage of the sodium sulfate absorption market and, mainly, due to tighter environmental protection regulations.

Taking care of these problems is giving a strong impulse to the development of new processes able to (1) produce caustic soda without chlorine generation using as a raw material mined sodium carbonate/bicarbonate with side production of pure carbon dioxide; (2) split salts (e.g. sodium sulfate and nitrate), which are available as by-products of different chemical processes, whilst caustic soda, acids or acid sodium

salts are recovered thus obtaining a "closed loop" process; (3) have a very low energy consumption for electrolysis in the range of 1700-2000 kWh/T of produced caustic soda; (4) produce a caustic soda with characteristics in the range of membrane chlor-alkali process.

De Nora Permelec has developed a technology which utilizes the hardware and operating concepts of the membrane electrolyzers for chlor-alkali production. The problem of energy saving is overcome by resorting to gas depolarized anodes fed by the hydrogen produced at the cathodes (Slides 46,47).

As already seen, the present technology comprises various kinds of depolarized electrodes, usually based on a porous substrate (e.g. carbon fabrics or felts, metal sheets sintered from powders or fibers, metal fabrics), provided on one face with a catalytic coating while the other side is made hydrophobic (Slide 48, left). Under optimum operating conditions the electrolyte partially fills the pores forming the meniscus in the region of the electrode containing the catalyst. Operating conditions causing percolation of the electrolyte through the pores or loss of gas in the electrolyte should be avoided. For this reason, anodes of this type allow rather small pressure differentials between the electrolytic compartment and the hydrogen chamber. Besides this limitation, conventional electrodes are affected by the problems caused by the presence of the electrolyte in the pores in direct contact with the catalyst. Therefore, either crystallization phenomena are experienced leading to the destruction of the porous structure, or some poisoning of the catalyst can occur when the electrolyte contains heavy metals, even in traces. These problems are overcome by using a depolarized anode made of a porous sheet containing a catalyst, bonded or pressed against a cation-exchange membrane (Slide 48, right). The assembly formed by the

membrane and the porous catalytic sheet is in turn bonded or maintained pressed against a suitable current collector, such as an expanded metal or wire mesh. The dimensions of the voids in the expanded metal or wire mesh are preferably small in order to allow at the same time a good mechanical support of the membrane/porous sheet assembly and a homogeneous current distribution.

In the case of bulk production of caustic soda (Slide 46) the equipment, other than the electrolyzer, consists of a reactor for neutralizing the acid sodium sulfate by sodium carbonate/bicarbonate, a carbon dioxide recovery, drying, liquefaction system, an inorganic impurities purification system of the neutralized sodium sulfate solution to be sent to the electrolyzers. Obviously, hydrogen depolarized anode electrolysis requires the hydrogen treatment section (gas disengager, abatement of the entrained caustic soda mist). The caustic soda separated from hydrogen is sent to utilization at a concentration between 15% and 30% according to users requirements.

In the case of the recovery of caustic soda and acid from by-product salts, the discussion is limited to sodium sulfate (other by-product salts, such as sodium nitrate, ammonium sulfate, may be substantially treated in the same way). The scheme illustrated for sodium carbonate/bicarbonate remains unchanged for all those cases where on-site utilization of acid sodium sulfate solutions is possible. If recycling to the upstream production stages requires pure sulfuric acid, the electrolyzer structure has to be modified by the addition of anionic membranes (Slide 47) (the energy consumption with this configuration is higher, around 3000 kWh/T of produced caustic soda; the concentration of the sulfuric acid produced is about 15%, while the concentration of caustic soda will range between 15% and 30% according to the users requirements).

BIBLIOGRAPHY

The following books have been utilized for preparing these lectures and extracting figures and tables. They are also suggested for further reading on the topics discussed:

1. H.A. Liebhafsky, E.J. Cairns, Fuel Cells and Fuel Batteries, Wiley, New York, 1968 (A comprehensive survey of the main impetus to fuel cells period, when these conversion systems were considered as power sources for NASA's space programs).

2. P. Gallone, Trattato di Ingegneria Elettrochimica, Tamburini, Milano, 1973 (A complete treatise on electrochemical engineering, still extremely valid, unfortunately limited to Italian-reading people).

3. M.O. Coulter (Ed.), Modern Chlor-Alkali Technology, Society of Chemical Industry, London, Ellis Horwood Limited, Chichester, 1980 (Proceedings of the 1979 International Chlorine Symposium, dealing in the main with development of the traditional processes. In particular, there is a fascinating account of mercury cell development in one organization from the Castner-Kellner rocking cell to their latest 400 kA design).

4. J. O'M. Bockris, B.E. Conway, E. Yeager, R.E. White (Eds.), Comprehensive Treatise of Electrochemistry, Volume 3, Electrochemical Energy Conversion and Storage, Plenum Press, New York, 1981 (In this volume, the principles of electrochemical energy conversion (by B.V. Tilak, R.S. Yeo, S. Srinivasan) and storage (by K. Kordesch) are discussed in some detail, followed by several specific chapters which give a detailed account of important batteries and fuel cells (in particular by D. Berndt for lead-acid batteries and by E.J. Cairns for high temperature secondary batteries); a chapter on electrochemical power for transportation (by E.J. Cairns, E.H. Hietbrink) and a presentation of the hydrogen economy (by J.O'M Bockris) are included).

5. U. Landau, E. Yeager, D. Kortan (Eds.), Electrochemistry in Industry: New Directions, Plenum Press, New York, 1982 (Invited plenary lectures presented at an international symposium by world-renowned experts of both the academic and industrial communities on the most important topics of industrial electrochemistry. The

following contributions are particularly relevant: Oxygen Electrodes for Industrial Electrolysis and Electrochemical Power Generation, by E. Yeager; Electrochemical Power Generation, by K. Kordesch; Batteries of the Future for Vehicle Applications, by E.J. Cairns).

6. E. Yeager, J. O'M. Bockris, B.E. Conway, S. Sarangapani (Eds.), Comprehensive Treatise of Electrochemistry, Volume 6, Electrodics: Transport, Plenum Press, New York, 1983 (In this volume, the transport aspects of electrochemical engineering are systematically covered. The chapter on porous electrodes (by Y.A. Chizmadzhev, Y.G. Chirkov) is particularly relevant).

7. C.A. Vincent with F. Bonino, M. Lazzari and B. Scrosati, Modern Batteries. An Introduction to Electrochemical Power Sources, Edward Arnold, London, 1984 (A clear book written for the non-specialist; the authors succeeded in maintaining a balance between describing well established "conventional" systems, and "state-of-the-art" developments which may or may not become of commercial importance).

8. R.E. White (Ed.), Eletrochemical Cell Design, Plenum Press, New York, 1984 (A collection of papers that were contributed to a national meeting, and that cover a wide range of electrochemical engineering topics. The following contribution is particularly relevant: Design Principles for Chlorine Membrane Cells, by K.H. Simmrock).

9. J.L. Sudworth, A.R. Tilley (Eds.), The Sodium Sulfur Battery, Chapman and Hall, London, 1985 (The most comprehensive and updated book covering all the aspects of this novel electrochemical system).

10. F. Hine, Electrode Processes and Electrochemical Engineering, Plenum Press, New York, 1985 (A comprehensive book on the most important topics of industrial electrochemistry and electrochemical engineering. The following chapters are particularly relevant: Voltage Balance and Energy Balance in an Electrolytic Cell; Fuel Cells and Application of Fuel Cell Concepts to Chemical Processes).

11. G. Prentice, Electrochemical Engineering Principles, Prentice Hall, Englewood Cliffs, 1991 (This volume describes the basic principles of electrochemical engineering and applies them to energy storage, electric

vehicles, chlor-alkali processes, etc.).

12. COMETT (Community Programme for Education and Training in Technology), Industrial Electrochemistry, Vol. II, Sintesi, Palermo, 1992 (A short training course. The following lectures are particularly relevant: Electrochemical Inorganic Processes, an Overview; The Electrolytic Production of Caustic Soda, Present Situation and Trends; Electrolyzer Design and Performances in Existing Technologies, Electrolyzers with a High Electrodic Surface to Volume Ratio, Membrane Electrolyzers, by G. Faita).

13. G. Bianchi, T. Mussini, Fondamenti di Elettrochimica: Teoria ed Applicazioni, Masson, Milano, 1993 (A concise and well-thought-out text-book of electrochemistry, unfortunately limited to Italian-reading people).

The following papers have also been utilized:

14. G. Clerici, M. Marchetto, Nuovi prodotti e tecnologie nel campo degli accumulatori al piombo, Rendiconti 84ª Riunione Annuale Associazione Elettrotecnica ed Elettronica Italiana, Cagliari, Ottobre 1983, Memoria A.14.

15. B. Leonardis, M. Leonini, Celle a combustibile ad acido fosforico: stato dell'arte - attività in Ansaldo, Rendiconti 84ª Riunione Annuale Associazione Elettrotecnica ed Elettronica Italiana, Cagliari, Ottobre 1983, Memoria A.17.

16. A. Dufour, F. Galbiati, Pile a combustibile con carbonati fusi: sviluppi in Ansaldo, Rendiconti 84ª Riunione Annuale Associazione Elettrotecnica ed Elettronica Italiana, Cagliari, Ottobre 1983, Memoria A.18.

17. G. Saccenti, R. Tartarelli, C. Zeppi, Termodinamica delle celle a combustibile ad alta temperatura, Rendiconti 84ª Riunione Annuale Associazione Elettrotecnica ed Elettronica Italiana, Cagliari, Ottobre 1983, Memoria A.24.

18. P. Gallone, L. Giuffré, G. Modica, Developments in Separator Technology for Electrochemical Reactors, Electrochimica Acta 28 (10), 1299/1307 (1983).

19. J.H. Altseimer, F. Roach, J.M. Anderson, C.A. Mangeng, The Potential Application of Fuel Cells in the Chlor-Alkali Industry, Department of Energy Report DOE/MC/A146-1896, Los Alamos National Laboratory Report LA-10516-MS, August 1985.

20. J.B. Goodenough, Solid Electrolytes and Their Applications, La Chimica e l'Industria 70 (11) Supplemento, 2/14 (1988).

21. G. Clerici, Un vaporetto elettrico per Venezia, Elettrificazione (11), 96/99 (1989); Un anno di navigazione sul vaporetto elettrico di Venezia, Elettrificazione (3), 80/84 (1991).

22. A. Dufour, La produzione di energia elettrica mediante celle a combustibile, La Rivista dei Combustibili 44 (10), 268/279 (1990).

23. F.R. McLarnon, E.J. Cairns, The Secondary Alkaline Zinc Electrode, J. Electrochem. Soc. 138 (2), 645/664 (1991).

24. T. Hirota, N. Nakajima, Development of On-Site Fuel Cell Power Units: Fuel Cell Stacks, Fuji Electric Review 38 (2), 43/44 (1992).

25. K. Harashima, H. Enomoto, T. Nakanishi, Elementary Technology Development: Development of High Performance Cells, Fuji Electric Review 38 (2), 64/66 (1992).

26. D. Casati, V. Quinto, Realtà tecnologica e prospettive delle celle a combustibile: il programma dimostrativo ENI, CH_4 Energia Metano 9 (5), 14/23 (1992).

27. V. Cincotti, D. Sardone, M. Sparacino, Progetto PRODE: il primo impianto di potenza con celle a combustibile ad acido fosforico in Europa, Atti Seminario "Pile a Combustibile", Associazione Italiana di Metallurgia, Milano, Dicembre 1992.

28. C. Mantegazza, G. Faita, L. Caprile, M. Casiglia, I sistemi a SPEFC per trazione elettrica, Atti Seminario "Pile a Combustibile", Associazione Italiana di Metallurgia, Milano, Dicembre 1992.

29. G. Bianchi, Le pile a combustibile come macchine elettrochimiche, Atti Seminario "Pile a Combustibile", Associazione Italiana di Metallurgia, Milano, Dicembre 1992.

30. G. Brusaglino, Towards a Commercial Market for Electric Vehicles and Boats, Proceedings of the Eleventh International Lead Conference (Pb 93), European Lead Development Committee, Venice, May 1993, Paper 5.3.

31. J.M. Stevenson, A.M. Lurshay, The Current Status of the Advanced Lead Acid Battery Consortium's (ALABC's) Research Programme, Proceedings of the Eleventh International Lead Conference (Pb 93), European Lead Development Committee, Venice, May 1993, Paper 7.5.

32. G. Faita, Caustic Soda without Chlorine Production, Electrosynthesis 7th International Forum on Electrolysis in the Chemical Industry, Florida, November 1993.

33. R. Wurster, Status of the Euro-Quebec Hydro-Hydrogen Pilot Project (EQHHPP), Workshop "Hydrogen as a Means of Energy Storing", Politecnico di Milano Dipartimento di Energetica, Milano, Novembre 1993.

34. A. Dufour, B. Marcenaro, Demonstration Projects for the Use of Hydrogen in the Automotive Field: Ansaldo European Initiatives, Workshop "Hydrogen as a Means of Energy Storing", Politecnico di Milano Dipartimento di Energetica, Milano, Novembre 1993.

35. C. Mantegazza, B. Marcenaro, SPFC System Integration: the De Nora Permelec Case, Royal Swedish Academy of Engineering Sciences, Stockholm, February 1994.

36. De Nora Permelec, Hydrina^{R} Membrane Electrolyzers, Brochure, 1994.

Glossary (C.A. Vincent et al., from Reference 7)

activation overpotential (overvoltage): Contribution to the total overpotential due to the charge transfer step at the electrode interface.

active mass: The material in an electrochemical cell which takes part in the cell reaction. For example, the lead oxide contained in the positive plate of a lead–acid battery.

anode: The electrode at which oxidation takes place, and which gives up electrons to the external circuit.

anolyte: The electrolytic phase in contact with the anode.

battery: An assembly of two or more cells electrically connected to form a unit. For example, a 12 V SLI battery is made up of six 2 V cells in series. However, the term is also often used to indicate a single cell.

binder: A polymeric material added to the active mass to increase its mechanical strength.

bipolar electrode: An electrode assembly which functions as the anode of one cell on one side, and as the cathode of the next cell on the other side. Also known as a 'duplex' electrode, especially in Leclanché batteries.

bus, bus bar: A rigid metallic conductor which connects different elements of a battery; also, the conductor for an electrical system to which a battery terminal is attached.

button cell: Miniature cylindrical cell having a characteristic disc shape.

can, case: The external envelope of a cell or battery, or the box containing the cells and connectors.

capacity, rated: The value of the output capability of a battery, expressed in Ah, at a given discharge rate before the voltage falls below a given cut-off value, as indicated by the manufacturer.

cathode: The electrode at which reduction takes place and which withdraws electrons from the external circuit.

catholyte: The electrolytic phase in contact with the cathode.

cell: Electrochemical device which directly interconverts chemical and electrical energy.

cell reversal: Inversion of the polarity of the terminals of a cell in a multicell battery. Cell reversal is usually due to overdischarge, when differences in

the capacity of individual cells result in one or more cells reaching complete discharge before the others.

charge acceptance: The ability of a secondary cell or battery to convert the active material to a dischargeable form. It is measured by the capacity which can be subsequently delivered to a load as a result of the charging process. If the charge acceptance is 100% then all of the electrical energy input would become available for useful output.

charge rate: See: C-rate.

charge retention: The ability of a charged cell to resist self-discharge.

charge, state of: The condition of a cell or a battery in terms of the remaining available capacity.

collector; current collector: Electronic conductor embedded in the active mass and connected to the bus bar or terminal.

concentration overpotential (overvoltage): Contribution to the total overpotential due to non-uniform concentrations in the electrolyte phase near the electrode surface caused by the passage of current.

corrosion: Oxidation of a metallic phase starting at the surface and caused by the reaction of the metal with components of the environment. In batteries corrosion phenomena play an important role especially in the case of primary aqueous cells and in high temperature systems.

C-rate: A method for expressing the rate of charge or discharge of a cell or battery. A cell discharging at a C-rate of r will deliver its nominal rated capacity in 1/rh; e.g. if the rated capacity is 2Ah, a discharge rate of C/1 corresponds to a discharge current of 2A, a rate of C/10 to 0.2A, etc.

creep: The process by which liquid electrolytes, and in particular alkalies, can escape past rubber–metal or polymer–metal seals, or through minute cracks in a cell case or lid.

current density: Electric flux per unit area. It is generally defined in terms of the geometric or projected electrode area and is measured in $A\,m^{-2}$ or $mA\,cm^{-2}$.

cut-off voltage: Final voltage of a discharge or charge operation. In the case of discharge, it is chosen as the voltage value below which the connected equipment will not operate, or below which operation is not recommended because of the onset of irreversible processes in the cell. In the case of charge, it is selected to allow complete conversion of active material with a minimum of gassing.

cycle: Sequence of charge and discharge of a secondary battery.

cycle life: The total number of charge/discharge cycles that can be delivered by a secondary cell or battery, while maintaining a predetermined output capacity and cycle energy efficiency.

depolariser: A substance which is supposed to reduce electrode polarisation.

The term was introduced when it was believed that the electrode polarisation was due solely to gas evolution at the electrode and the action of the depolariser was to eliminate or prevent this process. Today views are different, but the term is still sometimes used, usually to denote the positive active material.

discharge curve: A plot of cell or battery voltage as a function of time, or of discharge capacity, under a defined discharge current or load.

discharge depth: The percentage of the capacity to which a cell or battery has been discharged. Shallow/deep discharge: small/large fraction of the usable capacity consumed.

discharge rate: See: C-rate.

drain: Withdrawal of current from a cell or battery.

dry cell: A cell in which the electrolyte is immobilised, being either in the form of a paste or gel or absorbed in a microporous separator material.

dry charged cell: A cell which is in its fully charged state but without electrolyte.

duplex electrode: Type of electrode system used in flat Leclanché multicell batteries, formed by zinc coated on one side with carbon. It acts as the cathode current collector for one cell and as the anode for the adjacent cell. (see 'bipolar electrode').

electrode: The electronic conductor and associated active materials at which an electrochemical reaction occurs.

electrodeposition: Deposition of a chemical species at the electrode of an electrolytic cell caused by the passage of electric current.

electrolysis: Chemical modifications (i.e. oxidation and reduction) produced by passing an electric current through an electrolyte.

electrolyte: The medium which permits ionic conduction between positive and negative electrodes of a cell. It may be solid or liquid. In some cases the electrolyte may take part in the cell reaction.

equalising charge: Passage of an amount of charge by which the undercharged cells of a battery are brought up to a fully charged condition without damaging those already fully charged.

expander: A substance added in small amount to the active materials of a lead–acid battery to improve the service life and capacity of the electrodes. In particular, an expander prevents the increase in crystal grain size of lead in the negative electrode.

failure: The state in which the performance of a cell or battery does not meet the normal specifications.

float charging: Method of recharging in which a secondary battery is continuously connected to a constant voltage supply that maintains the cell in fully charged condition.

forming; formation: A series of charge/discharge cycles carried out under carefully controlled conditions after the manufacture of a secondary cell in order to optimise the morphology of the active mass.

fuel cell: An electrochemical generator in which the reactants are stored externally and may be supplied continuously to the cell.

gassing: Gas evolution which takes place towards the end of the charging of a battery.

grain boundary: The surface separating two regions of a solid having different crystal orientations.

grid: The lead framework of a lead–acid battery plate which holds the active material in place.

group: A set of electrodes within a cell which are connected in parallel.

hybrid cell: Electrochemical cell in which one of the two active reagents is in the gas phase and may be supplied from an external source. A hybrid cell occupies an intermediate position between closed cells and fuel cells.

hybrid electric vehicle: A vehicle that has more than one type of power supply to support the drive: e.g. battery/motor plus fossil fuel/internal combustion engine.

immobilised electrolyte: See: dry cell.

inhibitor: A substance added to the electrolyte which prevents an electrochemical process, generally by modifying the surface state of an electrode. A well known example is that of corrosion inhibitors which prevent metal corrosion.

initial drain: Current that a cell or battery supplies when first placed on a fixed load.

internal resistance: Resistance to the flow of direct current within a cell, causing a drop in closed circuit voltage proportional to the current drain from the cell.

iR loss; iR drop: Decrease in the voltage of a cell during the passage of current due to the internal resistance of the bulk phases within the cell – mainly that of the electrolyte and the separators. Also known as 'ohmic loss'.

load: The external devices or circuit elements to which electric power is delivered by a cell or battery.

load levelling: The intervention aimed at reducing non-uniform conditions in electricity demand. The principle of load levelling is to store energy when demand is low and to use it to meet peak demand.

loss: See: *iR* loss; polarisation loss.

maintenance: The procedures which are required in order to keep a battery in proper operating conditions. They may include trickle-charging to compensate for self-discharge, addition of water to the electrolyte, etc.

mass transport: Transfer of materials consumed or formed in an electrode process to or from the electrode surface. Mechanisms of mass transport may include diffusion, convection and electromigration.

negative: Negatively charged electrode, usually of a secondary cell; acts as anode during discharge and cathode during charge.

ohmic loss: See: *iR* loss.

open circuit voltage: The voltage of a cell or battery under no-load condition, measured with a high impedance voltmeter or potentiometer.

overcharge: The continued application of charging current to a cell or battery after it has reached its maximum state of charge.

overdischarge: Forced discharge of a cell or a battery past 100% of the available capacity. In the case of a multicell battery, the overdischarge may cause cell reversal.

overpotential; overvoltage: Difference between the actual electrode voltage when a current is passing and the equilibrium (zero current) potential. A number of different effects may contribute to the total overvoltage.

oxidation: The loss of electrons by a chemical species.

passivation: Surface modifications of metallic materials which cause an increase in their resistance to corrosion process.

passivity: The condition of a metallic material corresponding to an immeasurably small rate of corrosion.

plate: In the terminology of secondary batteries, this has the same meaning as 'electrode'.

polarisation: Deviation from equilibrium conditions in an electrode or galvanic cell caused by the passage of current. It is related to the irreversible phenomena at the electrodes (electrode polarisation) or in the electrolytic phase (concentration polarisation).

polarisation loss: Reduction in the voltage of a cell delivering current from its equilibrium value.

positive: Positively charged electrode, usually of a secondary cell: acts as cathode during discharge and anode during charge.

post: See: terminal.

primary battery: A cell or battery whose useful life is over once its reactants have been consumed; i.e. one not designed to be recharged.

rate: See: C-rate.

recombining cell: A secondary cell in which provision has been made for the products of overcharge reactions to recombine so that no net change occurs to the composition of the cell system as a result of overcharging.

reduction: The gain of electrons by a chemical species.

reserve battery: In principle, any battery which will not deliver current in its

manufactured form until activated by a suitable procedure, e.g. by adding the electrolyte to the dry components (water activated cells or cells activated by addition of special electrolytes), or by raising the temperature of the cell (thermal batteries, where the electrolyte is generally a mixture of salts in the solid state at ambient temperature).

reversal: See: cell reversal.

secondary battery: storage battery: Cell or battery which can be recharged after discharge, under specified conditions.

self discharge: Capacity loss of a cell or battery under open circuit conditions due to chemical reactions within the cell.

self discharge rate: The rate at which a cell or battery loses service capacity when standing idle.

separator: Electrically insulating layer of material which physically separates electrodes of opposite polarity. Separators must be permeable to the ions of the electrolyte and may also have the function of storing or immobilising the electrolyte.

service life: Timescale of satisfactory performance of a battery under a specified operating schedule, expressed in units of time or number of charge/discharge cycles.

shedding: The process whereby poorly adhering active mass (generally in the positive plate of a lead–acid cell) falls from the grid to form a sludge (mud) on the floor of the cell.

shelf-life: Period of time a cell can be kept idle after manufacture without significant deterioration.

short-circuit: The condition when the terminals of a cell or battery are connected directly.

SLI battery: A battery of usually 12 V or 24 V used for starting, lighting and ignition in vehicles with internal combustion engines.

stack: An assembly of parallel plates.

storage battery: See: secondary battery.

surface active agent: A substance which modifies the behaviour of a phase by interacting with its surface. For example, in the case of lead–acid batteries, the morphology of the active materials deposited at the electrodes may be strongly affected by the addition of surface-active agents.

terminal: The external electric connections of a cell or battery; also known as 'terminal post' or 'post'.

thermal battery: A type of reserve cell which is activated by raising the temperature.

thermal management: The means whereby a battery system is maintained within a specified temperature range while undergoing charge or discharge.

thermal runaway: A process in which a cell undergoes an uncontrolled rise in temperature due to the passage of increasing current (on, say, short-circuit discharge or constant voltage charging) as the temperature rises.

trickle charging: Method of recharging in which a secondary cell is either continuously or intermittently connected to a constant current supply in order to maintain the cell in fully or nearly fully charged condition.

uninterruptable power supply (UPS): A power system which maintains current flow without even a momentary break, in the event of mains or generator failure.

vent: Valve mechanism which allows controlled escape of gases generated during charging, but prevents spillage of electrolyte.

voltage delay: Time interval at the start of a discharge during which the working voltage of a cell is below its steady value. The phenomenon is generally due to the presence of passivating films on the negative electrode.

wet cell: A cell in which the liquid electrolyte is free-flowing.

Tavola cronologica degli sviluppi dell'elettrochimica

Periodo	ELETTROCHIMICA IONICA	ELETTROCHIMICA ELETTRODICA	TECNOLOGIE ELETTROCHIMICHE	METODI ELETTROANALITICI	APPLICAZIONI BIOLOGICHE E MEDICHE	Note
Prima del 1800			Deposizione di metalli per spostamento da soluzioni. Protezione catodica di parti di navi.		Stimolazione nervosa per mezzo di una pila rame-ferro (Galvani, 1791)	
1800		Pila di Volta				
1800-1825	Migrazione a salti per spiegare la conducibilità delle soluzioni (Grotthus, 1805).	Decomposizione dell'acqua (Nicholson e Carlisle, 1800). Decomposizione degli alcali (Davy, 1807).	Deposizione galvanica dei metalli (Brugnatelli, 1800).			Telegrafo elettrochimico (Salvà, 1804). Natura elettrica del legame chimico (Berzelius, 1804). Relazioni tra elettricità e magnetismo (Oersted, 1819). Elettrodinamica (Ampère, 1820).
1825-1850	Fenomeni di dissociazione e di ricombinazione nelle soluzioni (Gay-Lussac, 1839).	Leggi di Faraday (1934). Pila di Grove (1834).				Telegrafo elettromagnetico (Morse, 1837). 1° Principio della Termodinamica (Joule, 1847; Helmholtz, 1847). 2° Principio della Termodinamica (Carnot, 1825; Clausius, 1850; Thomson, 1851).
1850-1875	Esistenza degli ioni in soluzione (Clausius, 1857). Velocità di migrazione degli ioni in soluzione (Hittorf, 1858).	Fenomeni elettrocapillari (Lippmann, 1873).	Accumulatori al piombo (Planté, 1860). Pila Leclanché (1867).		Elettrocardiogramma (Kolliker & Muller, 1856). Elettroencefalogramma (Caton, 1874).	Invenzione della dinamo (1865). Definizione di entropia (Clausius, 1865).
1875-1900	Mobilità indipendente degli ioni (Kohlrausch, 1879). Teoria di Arrhenius per le soluzioni di elettroliti deboli (1884). Equilibri degli ioni in soluzione (Ostwald, 1888).	Doppio strato elettrico (Helmholtz, 1879). Equazione di Nernst (1891). Energetica delle pile (Ostwald, 1894). Selettività delle reazioni elettroorganiche (Haber, 1898).	Elettrolisi alluminio (Héroult & Hall, 1896). Preparazione elettrochimica del fluoro (Moissan, 1886). Celle a diaframma per soda-cloro (Grienheim, 1884). Celle a mercurio per soda-cloro (Castner, 1894). Accumulatori alcalini (Edison, 1900)	Analisi conduttimetrica (Ponte di Kohlrausch).		Definizione dell'elettrone (Stoney, 1891). *Zeitschrift für Physikalische Chemie* (1887). *Ostwald: Trattato di Elettrochimica* (1894).

(G. Bianchi, T. Mussini, from Reference 13)

1900-1925	Potenziali di membrana (Donnan, 1911). Solvatazione ionica (Born, 1920). Struttura ionica dei cristalli (1920). Conducibilità dei sali fusi. Teoria di Debye & Hückel (1923). Teoria acido-base (Brönsted, 1923).	Dipendenza da T di ΔH-ΔG di una pila (Richards, 1902). Legge di Tafel (1905). Doppio strato elettrico (Gouy, 1910; Chapman, 1913).	Elettrolisi ignea del cloruro di sodio per la produzione di sodio (Downs). Deposizione elettroforetica della gomma. Produzione elettrolitica di zinco (1915).	Definizione di pH (Sörensen, 1909). Polarografia (Heyrovsky, 1922).		*Electrochemical Society* (1902). *Faraday Society* (1903). *Premio Nobel ad Arrhenius* (1903), *ad Ostwald* (1909), *a Nernst* (1920). 3° Principio della Termodinamica: Nernst (1906), Planck (1912).
1925-1950	Effetto Wien (1927). Struttura dell'acqua (Bernal & Fowler, 1933). Estensione della teoria acido-base (Lewis, 1938). Struttura e proprietà degli elettroliti solidi (Wagner).	Teoria degli elementi galvanici in corto circuito (Evans). Struttura del doppio strato elettrico (Grahame). Formulazione teorica della relazione potenziale-corrente (Erdey-Gruz, Volmer).	Batterie al mercurio (Ruben, 1942). Cromature galvaniche. Arricchimento elettrolitico di acqua pesante. Lucidatura elettrolitica dei metalli (Jacquet). Produzione elettrolitica di magnesio (Dow). Protezione catodica.	Elettroforesi (Tiselius). Elettrodo a vetro per pH.		*Premio Nobel a Debye* (1936). *Comitato Internazionale di Termodinamica e Cinetica Elettrochimica* (1949).
1950-1975	Struttura e proprietà dei sali fusi. Elettroliti solidi a struttura aperta (β-allumine e $RbAg_4I_5$). Membrane ioniche artificiali e naturali.	Trattazione quantomeccanica dei processi di elettrodo. Relazione tra struttura del doppio strato elettrico e cinetica dei processi di elettrodo (Frumkin). Elettrocatalisi. Processi di trasporto agli elettrodi.	Elettrodialisi (1950). Sintesi dell'adiponitrile. Lavorazione elettrochimica dei metalli. Verniciatura per elettroforesi. Batteria sodio-zolfo (Kummer e Webber, 1960). Pile a gas per applicazioni spaziali. Elettrodi non metallici a base di ossidi. Pile al litio.	Elettrodi ionoselettivi. Analisi dell'ossigeno e del carbonio nei metalli fusi. Analizzatori di ossigeno.	Stimolatore cardiaco (1974). Monitoraggio elettrocardiaco continuo.	*Premio Nobel a Heyrovsky* (1959). *Premio Nobel a Onsager* (1968).
dal 1975 ai giorni nostri	Membrane protoniche fluorurate ad alta conducibilità (1988).		Celle a membrana per soda-cloro. Elettrolisi di solfato di sodio. Produzione elettrolitica di soda caustica da carbonato di sodio minerale. Pile a combustibile ad acido fosforico (PAFC). Pile a combustibile a membrana polimerica (SPE-FC). Automobile elettrica.		Elettrocalcificazione ossea.	*Premio Nobel a Prigogine* (1977). *Premio Nobel a R. A. Marcus* (1992). Tecnologia dell'idrogeno.

Table 1

Desirable Characteristics of Systems for High-Performance Electrochemical Cells

Characteristic	Anode reactant	Cathode reactant	Electrolyte
Electronegativity	Low (~1)	High (>1.5)	—
Equivalent weight (g/g equiv.)	Low (<30)	Low (<30)	Low[a] (<30)
Conductivity (Ω^{-1} cm^{-1})	High (>10^{-4})	High (>10^{-4})	High (>1)
Electrochemical reaction rate (i_0, A/cm^2)	High (>10^{-3})	High (>10^{-3})	High (>10^{-3})
Solubility in electrolyte (mol %)	Low (<0.1)	Low (<0.1)	—
Mass transport rate (equiv/sec cm^2)	High (>10^{-4})	High (>10^{-4})	High (>10^{-4})

[a] A more important criterion for the electrolyte is low density.

SLIDE No. 1: E.J. Cairns, from Reference 4.

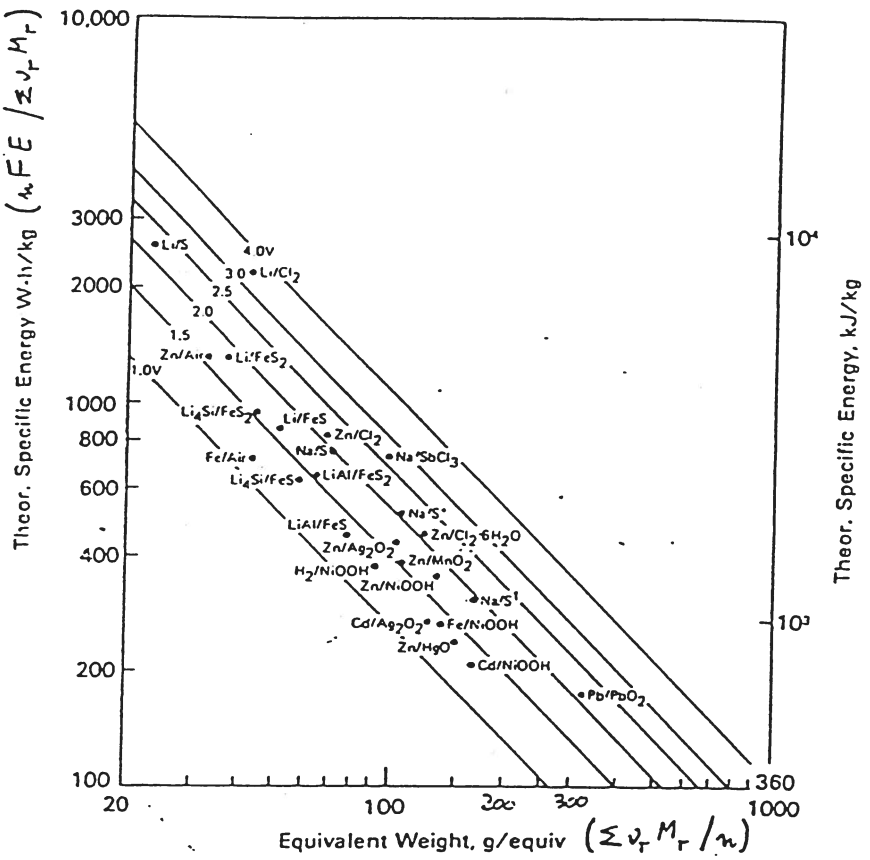

Figure 1. Theoretical specific energy (Wh/kg) for various electrochemical couples plotted against the sum of the molecular weights of the reactants times the number of moles of each involved in the balanced cell reaction. The straight lines are iso-emf lines. A good approximation to practical specific energies is obtained by multiplying the values in the figure by 0.2–0.25 for couples with solid reactants, and 0.15–0.2 if gaseous reactants are involved. Na/S* signifies $2Na + 5.2S \rightarrow Na_2S_{5.2}$, two-phase region; Na/S† signifies $Na_2S_3 + 2.2S \rightarrow Na_2S_{5.2}$, single-phase region.

SLIDE No.2: E.J. Cairns, from Reference 4.

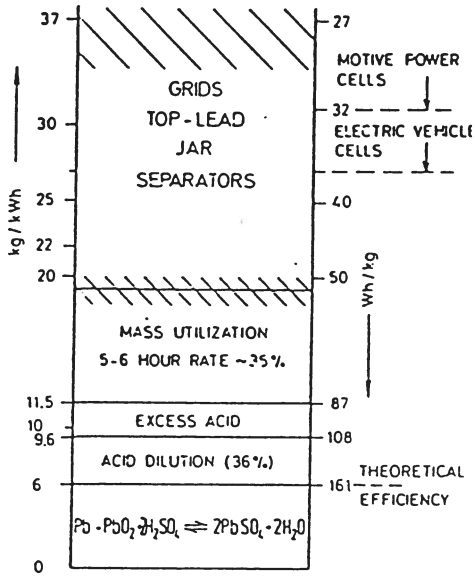

Figure 4. Weight contributions of the different construction elements (example: motive power cell).

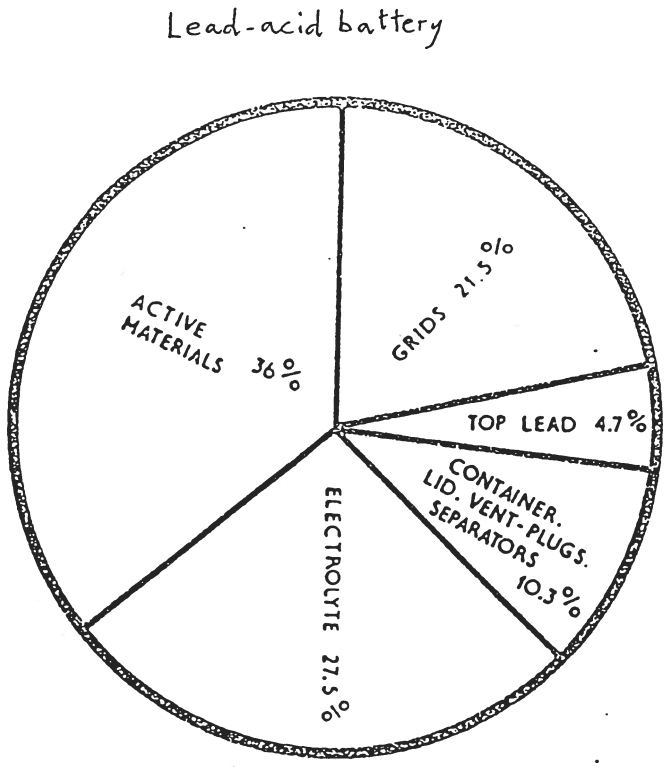

Figure 14. Weight analysis of a typical SLI battery.

SLIDE No.3: D. Berndt, from Reference 4 (upper figure).

K. Kordesch, from Reference 4 (lower figure).

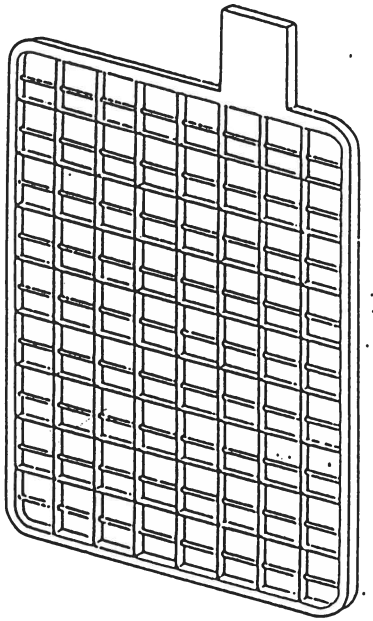

4.4 Typical lead–acid battery grid: this acts as a framework to hold the active material in place.

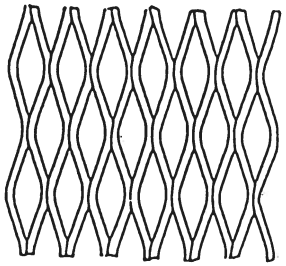

4.5 Expanded metal grid.

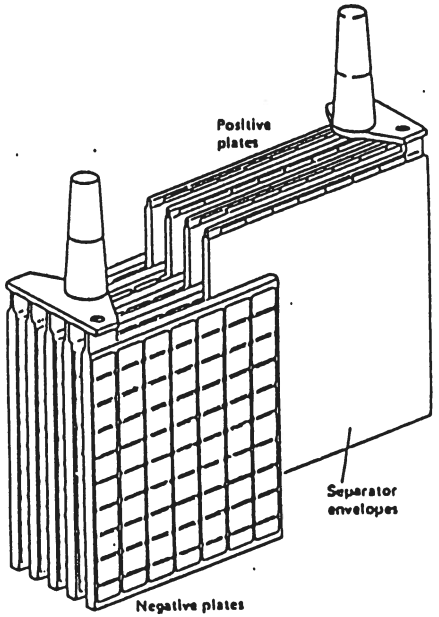

4.7 Interleaving of positive and negative electrode groups (elements) to form a lead–acid cell.

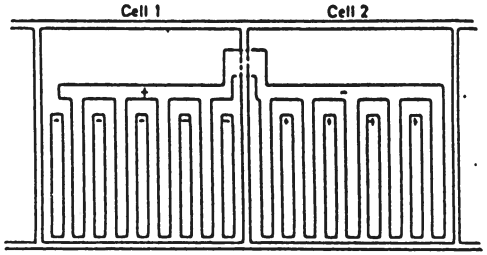

4.8 Schematic diagram of lead–acid battery showing through-partition connection.

SLIDE No. 4: F. Bonino, C.A. Vincent, from Reference 7.

Schema di produzione delle piastre con la nuova tecnologia

MAGNETI MARELLI

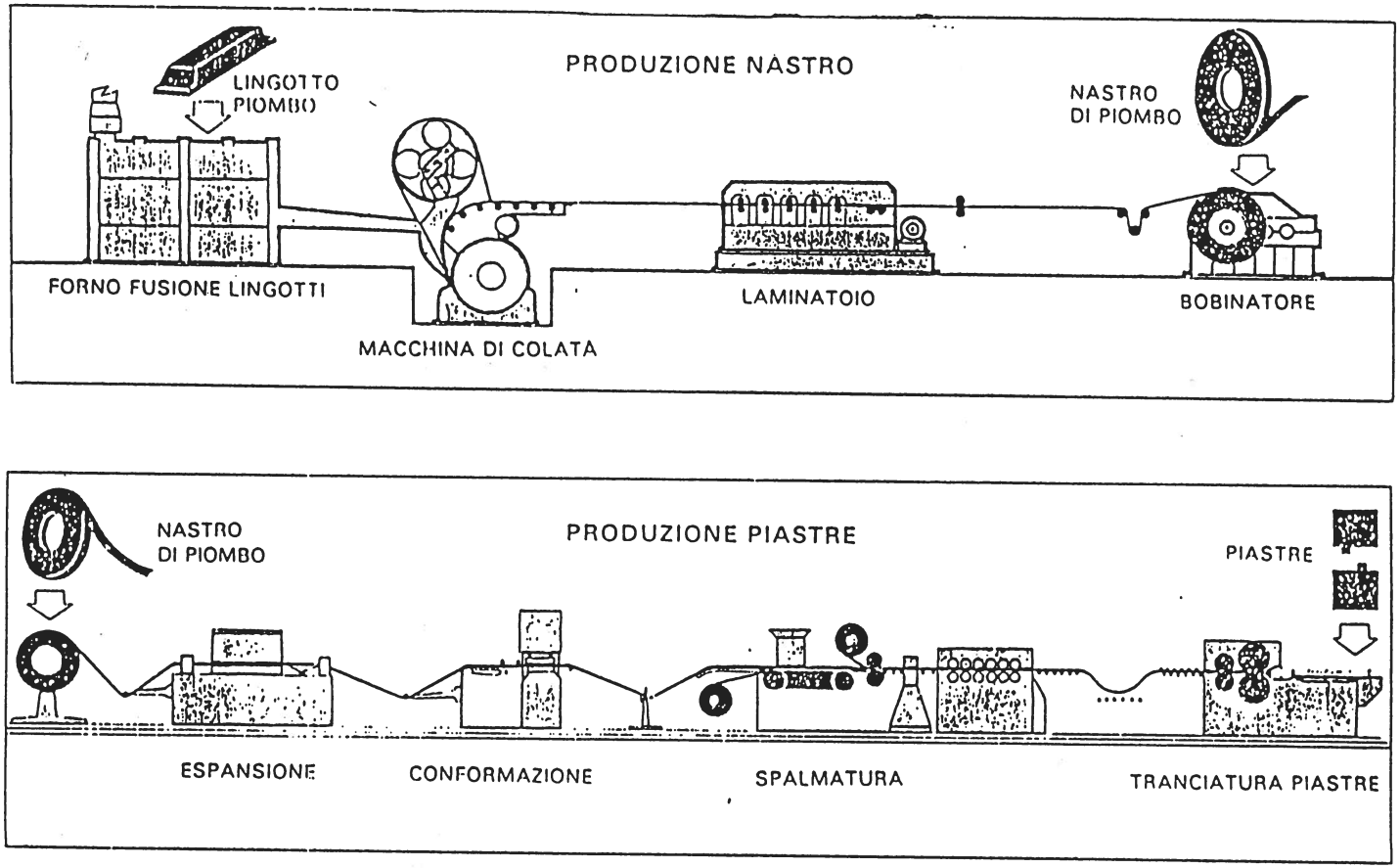

SLIDE No. 5: G. Clerici, M. Marchetto, from Reference 14.

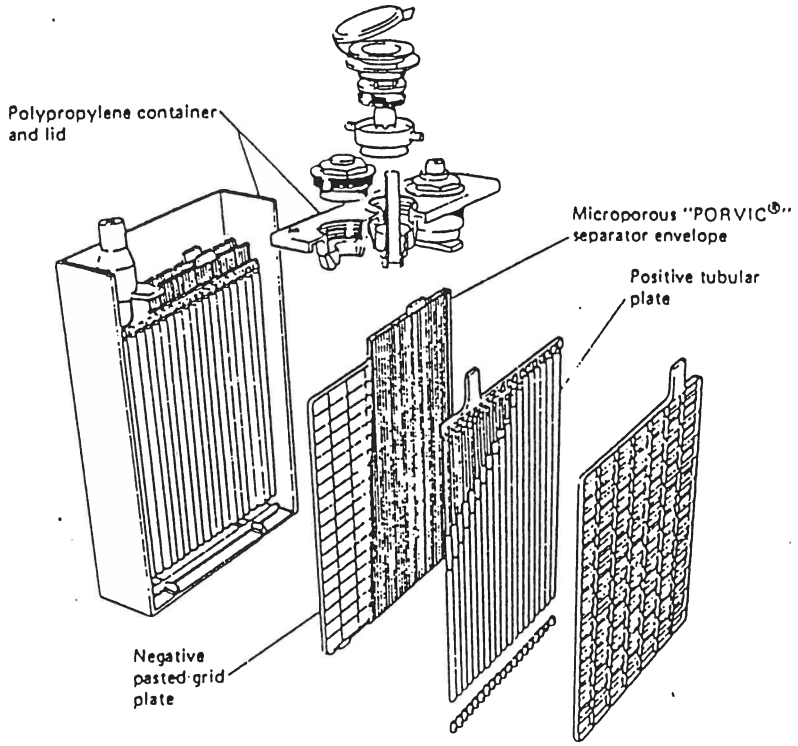

4.13 Motive power lead–acid cell with tubular positive plates in which the active material is contained in pre-formed terylene tubes, and negative pasted grid plates surrounded by micro-porous polyvinyl chloride separator envelopes. The case and lid are formed of heat sealed polypropylene. (By courtesy of Chloride Industrial Batteries)

SLIDE No.6: F. Bonino, C.A. Vincent, from Reference 7.

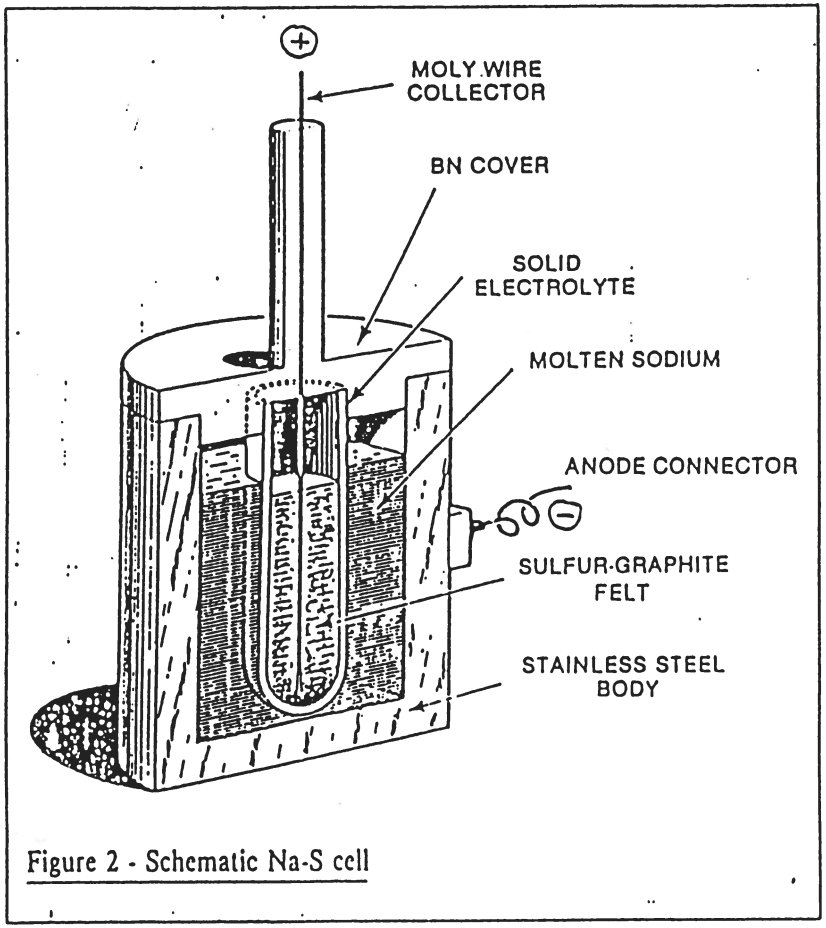

Figure 2 - Schematic Na-S cell

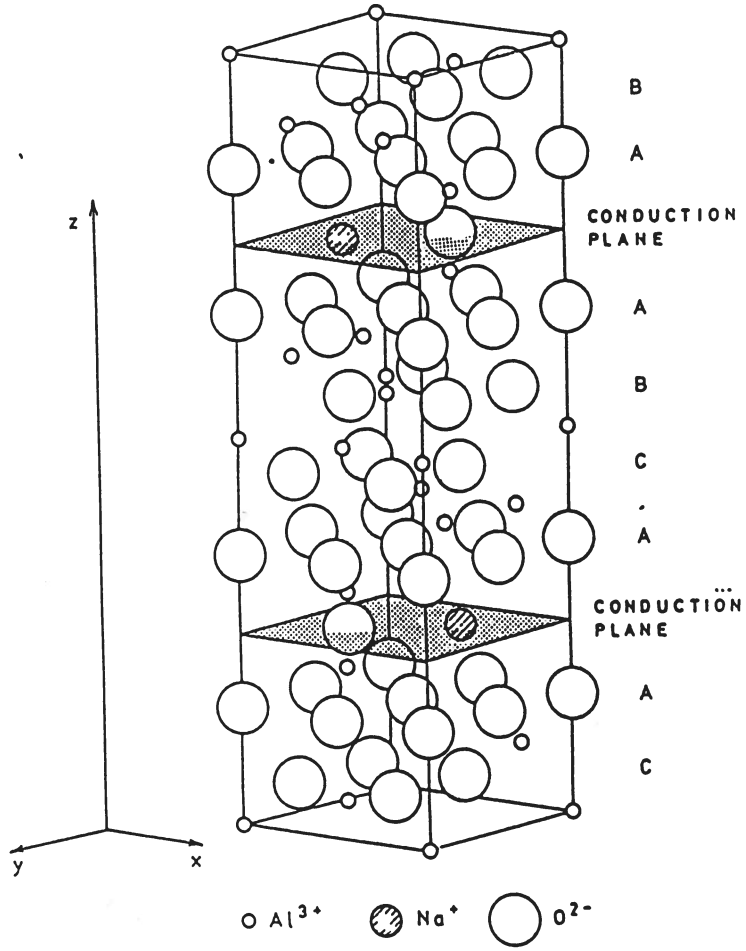

Fig. 2.1 Perspective drawing of the idealized structure of beta alumina ($Na_2O \cdot 11 Al_2O_3$)

SLIDE No.7:. J.B. Goodenough, from Reference 20 (figure on the left).
P.T. Moseley, from Reference 9 (figure on the right).

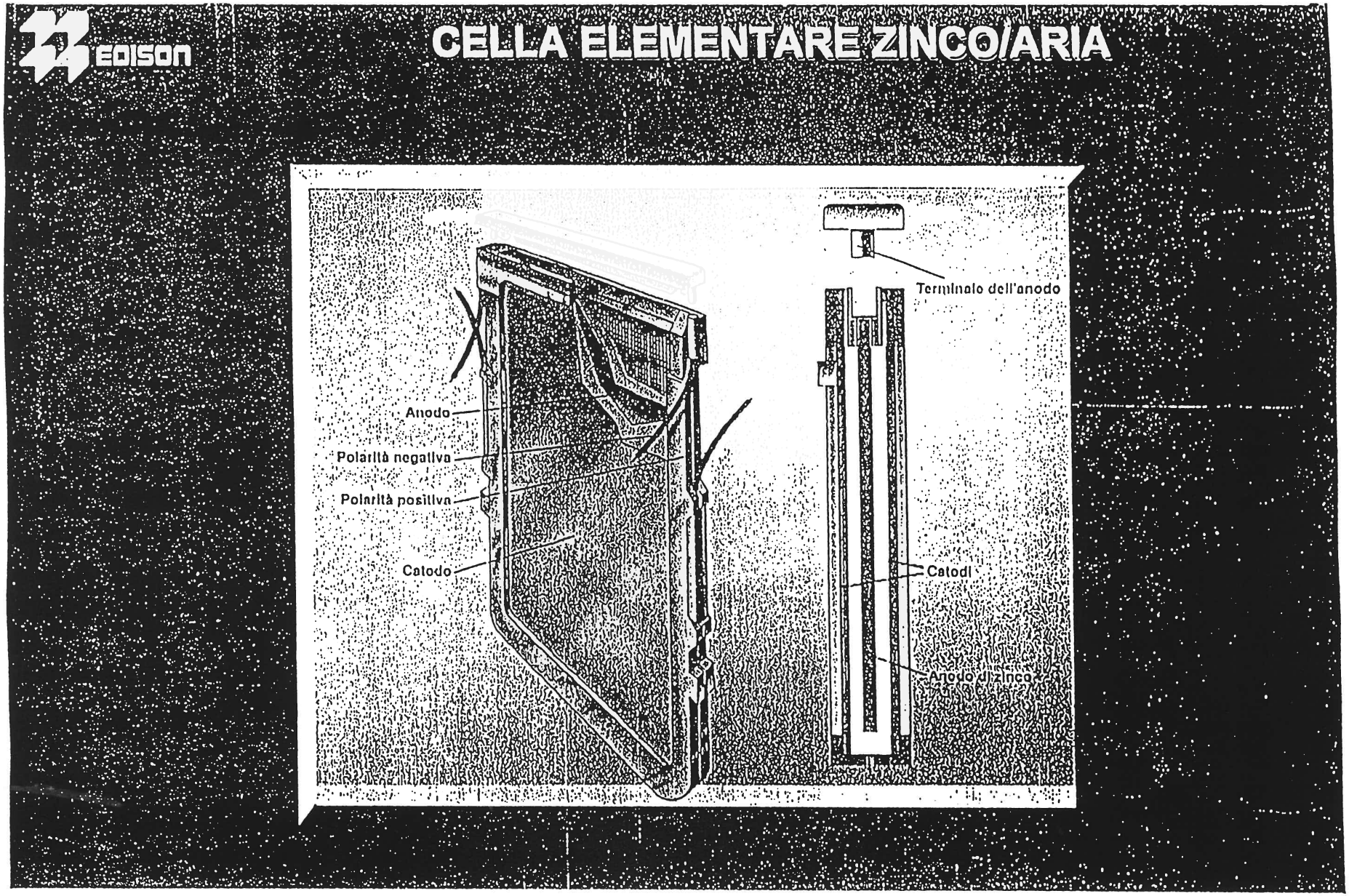

SLIDE No.8: by courtesy of Edison Termoelettrica S.p.A.

Table 27
Candidate Power Sources for Electric Vehicles

System	O/C Cell voltage	Theoretical, Wh/kg	Status						Remarks
			Wh/kg[a]	Wh/liter	W/kg[b]	Efficiency	Cycle[c] life	Range,[d] km	
$Pb-H_2SO_4-PbO_2$	2.1	175	20–40	45–90	80	70	300	35–65	Bench mark. Available now.
Fe-KOH-NiOOH	1.4	267	50	90	125	50–60	100 +[e]	85	Low efficiency, gassing.
Zn-KOH-NiOOH	1.7	373	75	140	150	75	200 +	125	Better cycle life needed.
$Zn-ZnCl_2-Cl_2$	2.1	461	70	~80	60		1000[f]	115	Complex, bulky, safety(?), maintenance.
$Zn-ZnBr_2-Br_2$	1.8	430	60	~60	75	65	200 +	100	Complex, bulky, safety(?)
Fe-KOH-air	1.2	720	90	~90	30	45	200	150	Low efficiency, bulky.
Zn-KOH-air	1.6	1310	70–90	70–90	80	35	MR[g]	115–150	Not rechargeable, bulky.
Al-NaOH-air	2.7	2790	N.A.[h]	N.A.	N.A.	~35	MR	—	Not rechargeable, low efficiency.
$Li-LiClO_4-TiS_2$	2.2	490	(120)[i]	(170)	(100)	~75	100 +	(200)	Safety(?) Cycle life(?)
LiAl-LiCl-KCl-FeS	1.3	458	50–90	75–130	60–100	~70	300 +	85–150	Thermal control needed.
$Li_4Si-LiCl-KCl-FeS_2$	1.8, 1.3	944	120	180	100	~75	700	200	Thermal control needed.
$Na-\beta-Al_2O_3-S$	2.0	758	85–140	100–165	60–130	~75	200–1500	140–235	Thermal control needed.
$H_2-H_3PO_4$-air	1.0	[j]	[j]	[j]	25–75	N.A.	40	400 +[k]	Complex, bulky, expensive.

[a] At 30 W/kg.
[b] Peak specific power, at least 15 sec.
[c] At least 80% DOD.
[d] 25% of vehicle test weight allocated to batteries. Urban driving profile, 0.15 kWh/km.
[e] Cycle lives of up to 1500 were demonstrated for earlier electrode designs.
[f] This cycle life for 1-kWh system with electrolyte maintenance.
[g] MR = mechanically rechargeable. The anodes are replaced periodically. Life data not available.
[h] N.A. = not applicable.
[i] Figures in parentheses are projections based on lab cells of low specific energy.
[j] Depends on amount of fuel carried—may be as high as ~ 6100, in principle.
[k] Typical range for fuel-carrying vehicle.

O/C = open-circuit
DOD = depth of discharge

SLIDE No. 9: E.J. Cairns, E.H. Hietbrink, from Reference 4.

VEHICLE PROPULSION POWER CALCULATIONS

$$P_b = \frac{P_r}{E_m \cdot E_e} + \frac{P_a}{E_{ae}}$$

$$P_r = V(F_r + F_w + F_g + F_a)$$

$$F_r = M_v g K \ (1 + 0.022\ V)$$

$$F_w = \rho_a C_d A_f \frac{V^2}{2}$$

$$F_g = M_v g \sin \Theta$$

$$F_a = 1.1\ M_v \frac{dV}{dt}$$

P_b = power required from the battery, watts

P_r = power required at the rear wheels, watts

E_m = mechanical efficiency of the drive train (transmission, differential)

E_e = electrical efficiency of the drive train (power electronics, motor)

P_a = power required for the work of the accessories

E_{ae} = efficiency of the accessories

V = vehicle velocity, meters/second

F_r = rolling resistance of the tires, newtons

M_v = vehicle test mass, kg

g = gravitational constant, 9.807 meters/second^2

K = coefficient of rolling resistance for the tires (0.008-0.015)

F_w = wind resistance, newtons

ρ_a = density of air, kg/m^3 (1.2255 kg/m^3 at 15°C and 760 torr)

C_d = air drag coefficient for the vehicle, 0.3-0.7, depending on streamlining

A_f = frontal area of the vehicle, m^2

F_g = gravitational force, newtons

Θ = angle of inclination of road

F_a = acceleration force, newtons.

SLIDE No. 10: E.J. Cairns, from Reference 5.

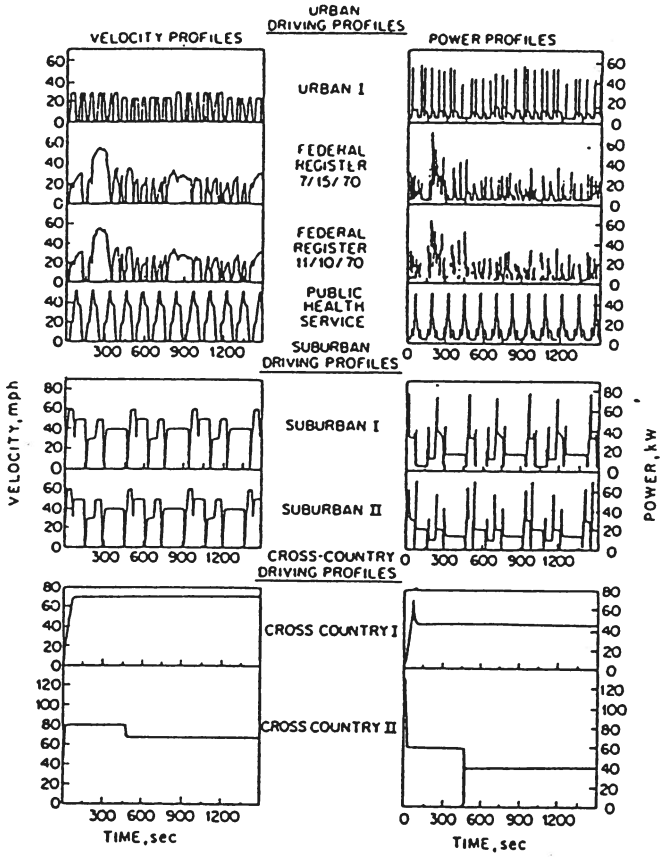

Figure 4. Sample driving profiles and corresponding power profiles (for a 1700 kg automobile). (3)

SLIDE No. 11: E.J. Cairns, from Reference 5.

Table I. Energy and Power Requirements for Urban Electric Vehicle

Energy Consumption*	
At Axle	0.10-0.12 kW·h/T·km
From Battery	0.14-0.17 kW·h/T·km
From Plug	0.18-0.23 kW·h/T·km
Peak Power Required (0 to 50 km/h, ≤ 10 s)	
At Axle	25 kW/T (Test Wt.)
From Battery	35 kW/T (Test Wt.)

Average Power Required

	At Axle	From Battery
Urban Driving (Avg. 32 km/h)	3-3.5 kW/T	4-5 kW/T
50 km/h Cruise	3-3.5 kW/T	4-5 kW/T

*These energy consumption figures correspond to urban driving profiles such as the Federal Register driving profile, and represent an average speed of about 32 km/h.

SLIDE No. 12: E.J. Cairns, from Reference 5.

$$R = \frac{S_pE \cdot f_b}{0.15}$$

R = vehicle range under urban driving conditions, km

S_pE = specific energy of the battery, Wh/kg

f_b = fraction of the vehicle test mass assigned to battery

0.15 kWh/T.km = 0.15 Wh/kg.km of vehicle mass = average road load energy required from batteries (urban driving profile)

For R = 150 km and f_b = 0.3, S_pE must be 75 Wh/kg

SLIDE No. 13: E.J. Cairns, from Reference 5.

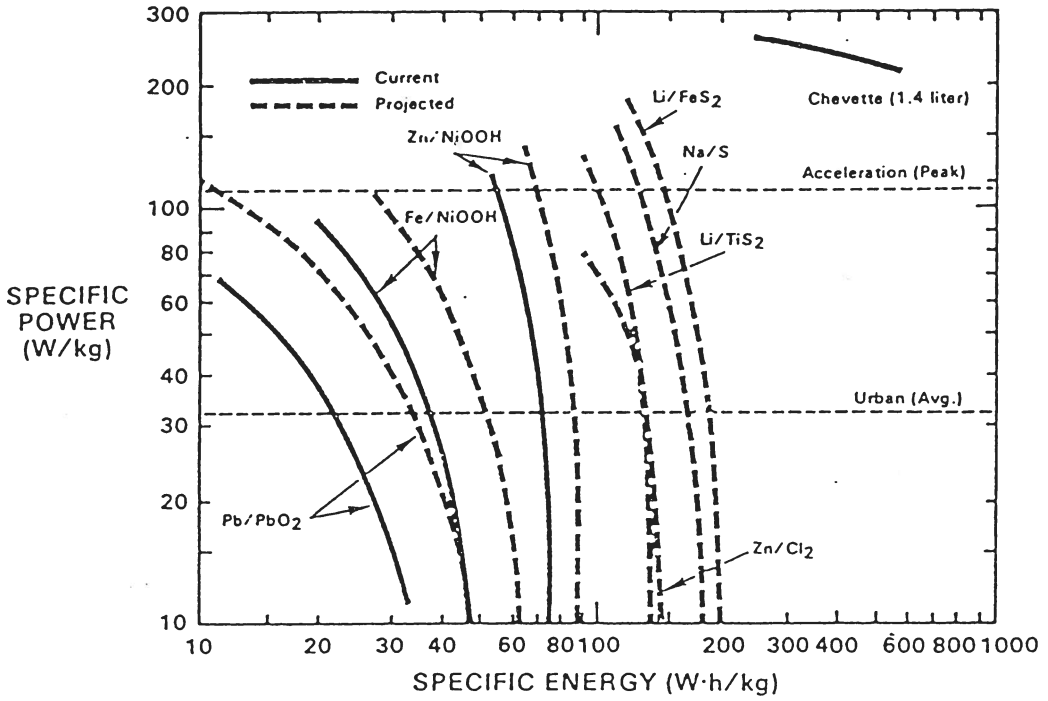

Figure 34. Specific power vs. specific energy for electric vehicle battery candidates.[50,70,76,90,85,128,129]

SLIDE No. 14: E.J. Cairns, E.H. Hietbrink, from Reference 4.

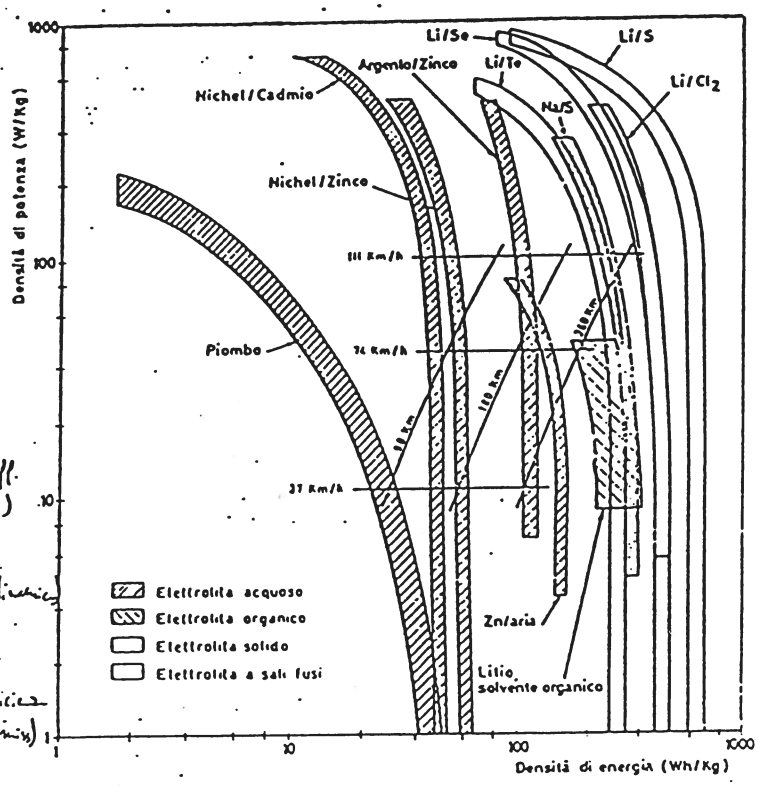

$M_v = 900$ kg

$f_b = \frac{225}{900} = 0,25$

$K = 0,0175$ (coeff. attrit. volvente)

$C_d = 0,6$ (coeff. resistenza aerodinamica)

$A_f = 2\ m^2$

$E_m \cdot E_c = 0,75$ (efficienza sist. motore + trasmiss.)

FIG. 7 - Caratteristiche operative di alcune batterie. Per confronto sono riportate le caratteristiche richieste alla sorgente di energia da un utilizzatore

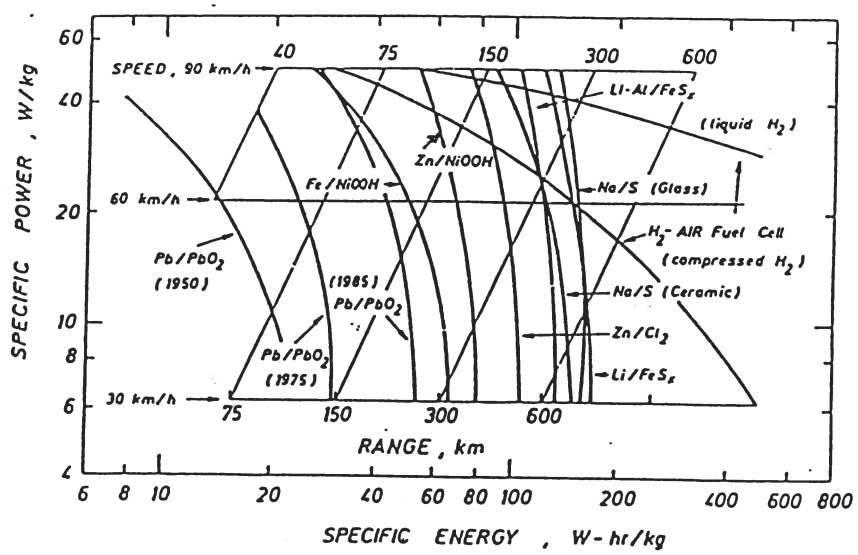

Figure 13. Specific power and specific energy diagram for the lead–acid battery and advanced systems. A grid of the projected ranges of a 1300-kg automobile with a 300-kg battery at different speeds is drawn in.

SLIDE No. 15: K. Kordesch, from Reference 4 (lower figure).

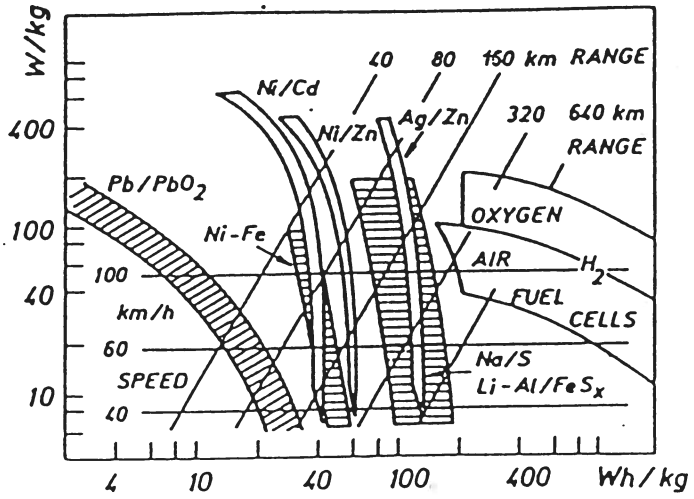

Fig.7: Comparison of different battery systems. The energy density is shown as a function of the power output/kg needed to propel a ~1000 kg electric vehicle at a fixed certain speed over a required range. Battery-wgt.: 300 kg

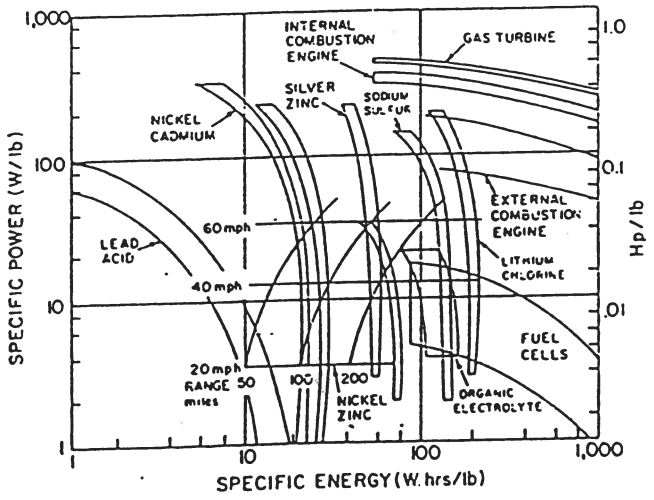

Figure 36. Specific power vs. specific energy for various energy producers.[137]
(1 mile ≃ 1.6 km; 1 lb ≃ 0.45 kg; 1 Hp ≃ 0.745 kW)

SLIDE No. 16: K. Kordesch, from Reference 5 (upper figure).
B.V. Tilak , R.S. Yeo, S. Srinivasan, from Reference 4 (lower figure).

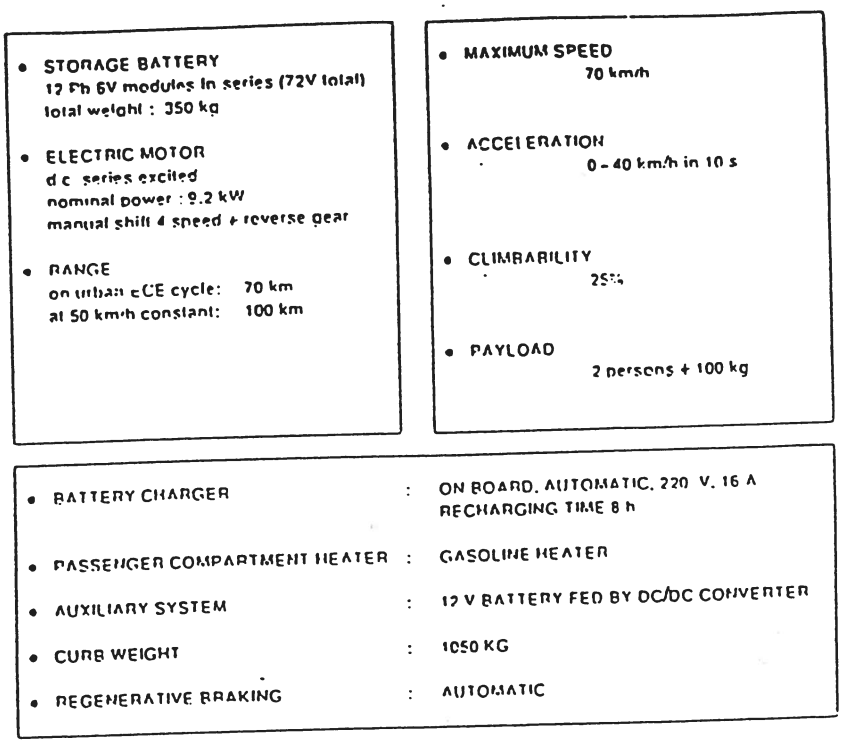

FIG. 3 - MAIN CHARACTERISTICS OF FIAT PANDA ELETTRA

Table 5
Near-Term DOE Electric Vehicle Performance Objectives[a]

Minimum passenger capacity	Four adults
Maximum curb weight	Open
Minimum urban range, km	121
Maximum electric recharge energy in urban driving, kWh/km	0.32
Maximum recharge time, h	6
Safety features	Meet federal motor vehicle safety standards
Minimum ambient temperature range, °C	−29 to + 52
Minimum top speed, km/h	97
Maximum acceleration time, sec (0–48 km/h)	9
Maximum merging time, sec (40–89 km/h)	18

[a] Reference 48 (1979)

SLIDE No. 17: G. Brusaglino, from Reference 30 (upper table).
E.J. Cairns, E.H. Hietbrink, from Reference 4 (lower table).

Utility vehicle, used in the U.S. Postal Service

Table 6
AM General DJ-5E Design and Performance Characteristics

GVM[a], kg	1955
Payload, kg	306
Battery mass, kg	586
Cargo space, m^3	1.7
Acceleration time, sec (0–48 km/h)	20
Gradability	
Speed on 10% grade, km/h	22.4
Range, km	
Constant speed of 48 km/h	48
Postal cycle	40
Energy consumption, Wh/kg km	0.4–0.5

1979

[a] GVM = gross vehicle mass

Delivery and service van

Table 7
GMC Design and Performance Characteristics[a]

GVM[b], kg	3682
Payload, kg	682
Battery mass, kg	1137
Lead-acid battery mounting	Single pack under vehicle
Safety	Full FMVSS[c] compliance
Drive train	Direct current series motor with chain drive gear reduction and solid state continuous electronic speed control
Brakes	Vacuum assisted hydraulic with electrical regeneration
Acceleration time, sec (0–48 km/h)	12
Grade limit, %	20
Top speed, km/h	80
Range on SAE J227a "C," km	64

[a] From Reference 53 (1979). General Motors Corporation

[b] GVM = gross vehicle mass
[c] FMVSS = federal motor vehicle safety standards

SLIDE No. 18: E.J. Cairns, E.H. Hietbrink, from Reference 4.

Tabella I.6 Caratteristiche e prestazioni tipiche di una vettura con motore a scoppio di media cilindrata

Numero di cilindri	4	Cilindrata totale	1200 cm^3
Velocità massima	120 km/h	Potenza massima	50 CV = 36,8 kW (*)
Velocità normale	90 km/h	Potenza normale	20 CV = 14,7 kW
Serbatoio carburante	40 l	Autonomia a velocità normale (con sviluppo di energia 66 kWh) (**)	400 km (4,5 ore)
Peso a vuoto (di cui circa 1/3 = peso apparato motore)	950 kg	Portata utile	300 kg

(*) 1 CV = 0,745 kW

(**) Per ottenere la stessa autonomia occorrerebbero 2200 kg di batterie al Pb (30 Wh/kg)

SLIDE No. 19: P. Gallone, from Reference 2.

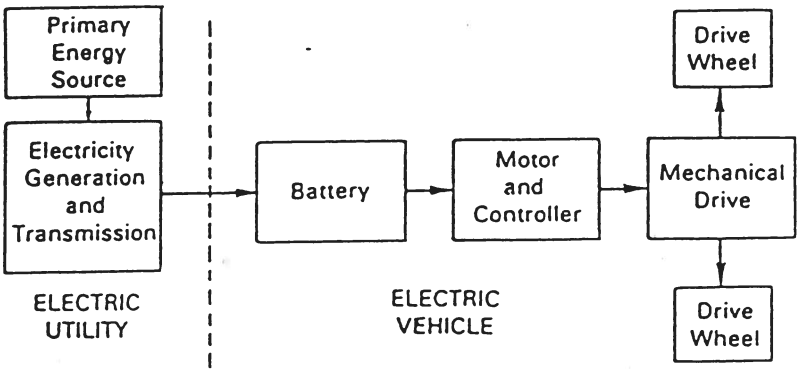

Figure 1. Electric vehicle schematic.

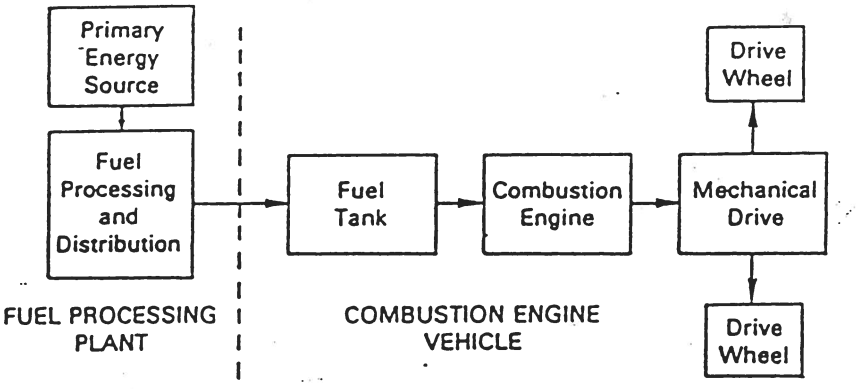

Figure 2. Combustion engine vehicle schematic.

SLIDE No. 20: E.J. Cairns, E.H. Hietbrink, from Reference 4.

ACTV VENEZIA

Tabella 1 - Principali caratteristiche del vaporetto elettrico

— lunghezza:	23 m
— larghezza:	4,22 m
— altezza:	1,9 m
— stazza lorda:	25 t
— portata passeggeri:	210
— scafo in lega leggera:	alluminio-magnesio
— batteria:	240 V — 1450 Ah
— convertitore:	c.c./c.a. a frequenza variabile
— motore elettrico asincrono trifase:	60 kW
— elica-timone azimutale (consente la massima manovrabilità)	

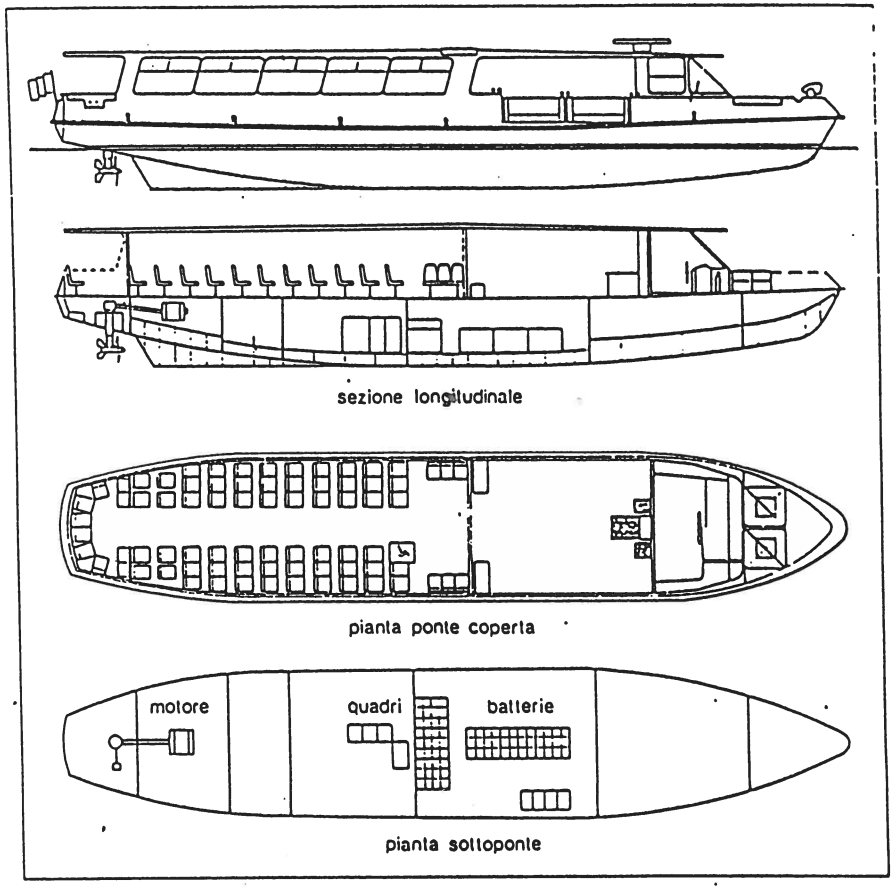

Fig. 2 - Sezione e pianta del battello.

SLIDE No. 21: G. Clerici, from Reference 21.

Tabella 2 - Caratteristiche delle batterie Magneti Marelli

	Batteria trazione	Batteria ausiliaria
Tipo Numero Capacità Peso Peso complessivo	elemento HK 21 120 elementi da 2 V 1450 Ah/5 h 86 kg 11 tonnellate	batteria 6 STV 13 6 batterie da 12 V 150 Ah/10 h 39 kg 235 kg
L'impiego di elementi HK 23 a pari tensione (circa 13 tonnellate) può estendere il percorso fino al Lido. Gli elementi HK utilizzano piastre positive a tubetti da 10 mm		

ACTV VENEZIA

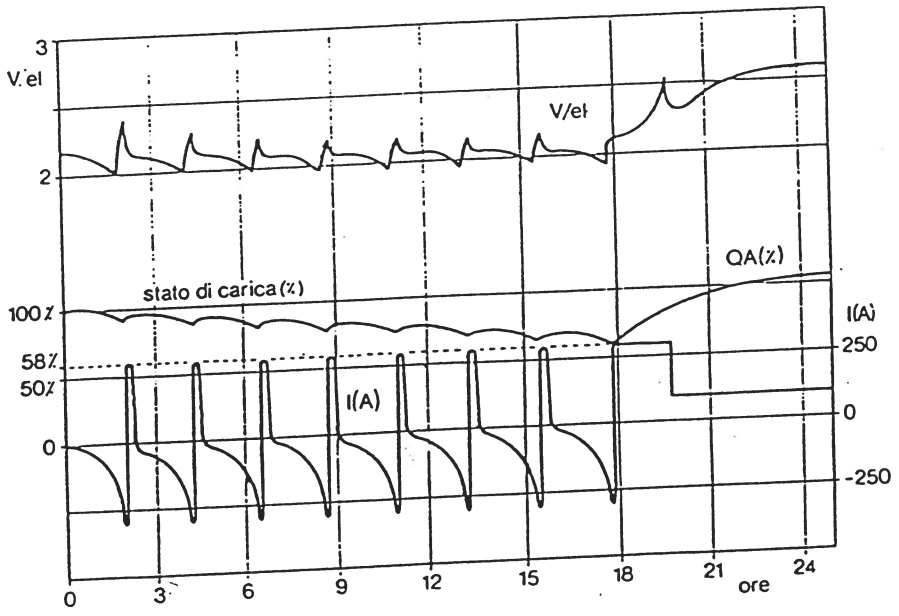

Fig. 4 - Andamento dello stato di carica della batteria durante il ciclo giornaliero.

SLIDE No. 22: G. Clerici, from Reference 21.

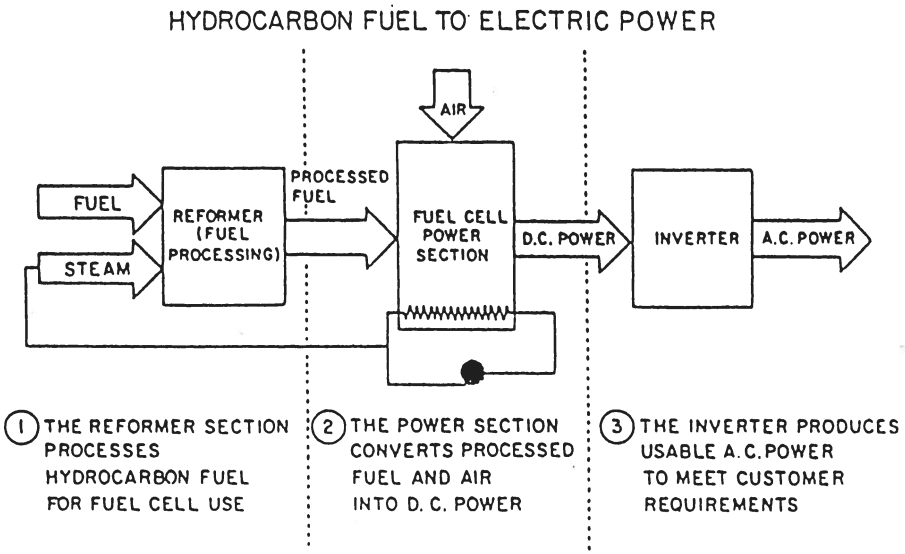

Figure 27. Basic segments of a typical fuel cell power plant.[122]

SLIDE No. 23: B.V. Tilak, R.S. Yeo, S. Srinivasan, from Reference 4.

Table 7
Components of Cells for Four Different Fuel Cells[119][a]

Fuel cell	Anode	Cathode	Electrolyte (thickness in mm)	Temperature of operation, °C	Cell voltage, V; current density, mA/cm²
Phosphoric acid	C catalyzed by Pt (1 mg/cm²)		99 wt % H_3PO_4 immobilized in a matrix (0.5)	190	0.8; 200
Alkaline	C catalyzed by Pt[b] (1 mg/cm²)	C catalyzed by Ag[b] (5 mg/cm²)	30 wt % KOH (0.5)	70	0.8; 100
Molten carbonate	Porous Ni	Lithiated NiO	Alkali aluminate + molten alkali carbonates (1.0)	650	0.7; 200
Solid electrolyte	Ni-ZrO_2 Cermet	In_2O_3-$PrCoO_{3-x}$ with Cr_2O_3 interconnection	$(ZrO_2)_{1-x}(Y_2O_3)_x$(0.04)	1000	0.84; 400

[a] Voltage degradation at constant power output: 5%; useful life: 36 months.
[b] Prospects are good for developing alkaline fuel cells with much lower noble metal loadings or with substitutes for noble metals as electrocatalysts.

SLIDE No. 24: B.V. Tilak, R.S. Yeo, S. Srinivasan, from Reference 4.

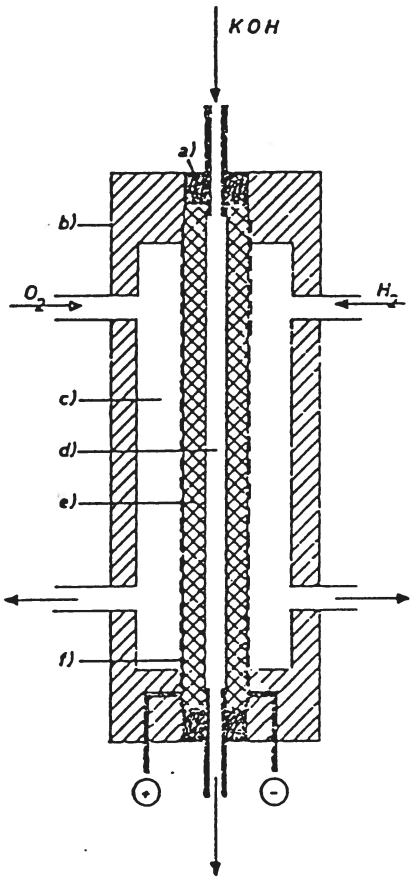

Fig. 43. Section of an individual hydrogen–oxygen cell with gas and electrolyte circulation: a, gasket; b, frame; c, gas chamber; d, electrolyte; e, porous metal plates; f, supporting grids as current collectors.

$$A)\ H_2 + 2OH^- = 2H_2O + 2e^-$$

$$C)\ \tfrac{1}{2}O_2 + H_2O + 2e^- = 2OH^-$$

$$H_2 + \tfrac{1}{2}O_2 = H_2O$$

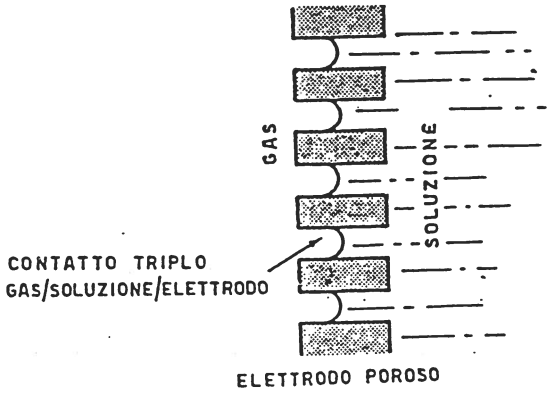

Fig. 26.5. Configurazione di un elettrodo poroso a gas.

SLIDE No. 25

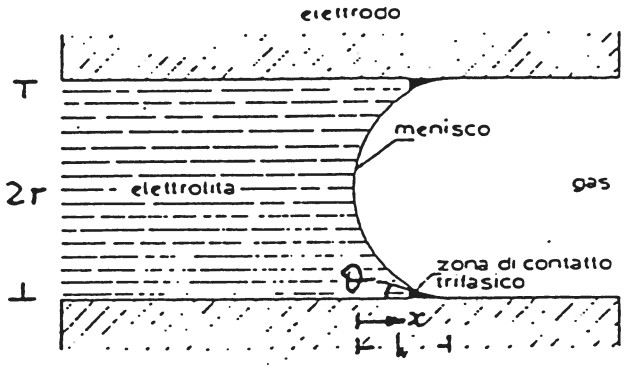

$$P_g - P_l = \Delta P = \frac{2\gamma \cos\theta}{r}$$

$$(\Delta P \cdot \pi r^2 = \gamma \cos\theta \cdot 2\pi r)$$

Fig. VI.10 – Elettrodo poroso: zona di contatto trifasico substrato-elettrolita-gas.

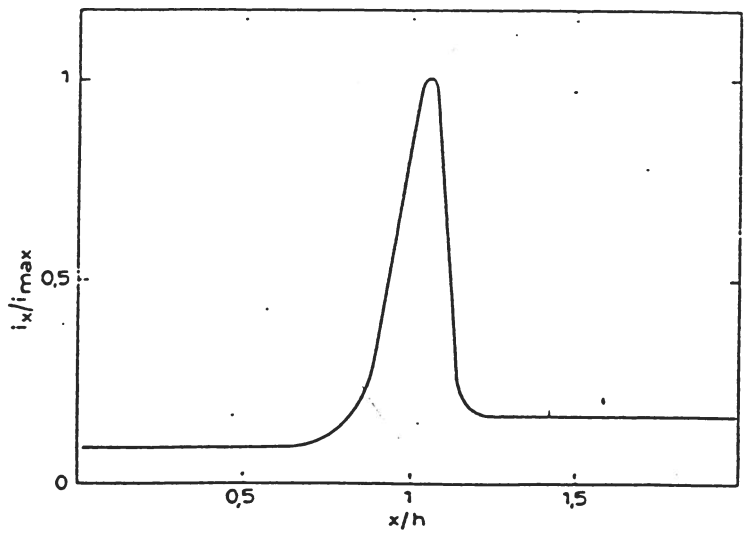

Fig. VI.11 – Distribuzione tipica della corrente di riduzione dell'ossigeno presso il menisco: x = distanza dalla base del menisco; h = altezza visibile del menisco; i_x = densità di corrente locale; i_{max} = densità di corrente massima.

SLIDE No. 26: P. Gallone, from Reference 2.

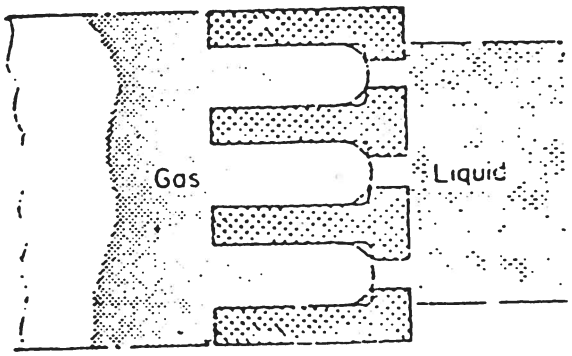

Fig. 17 Schematic cross-section of a bi-porous electrode.

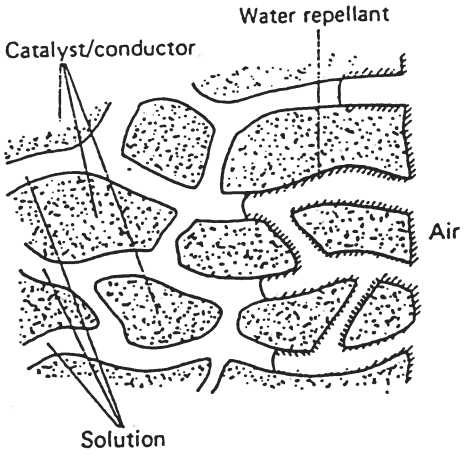

3.31 Schematic view of the interphase at a porous matrix air electrode.

SLIDE NO. 27: M. Lazzari, from Reference 7 (lower figure).

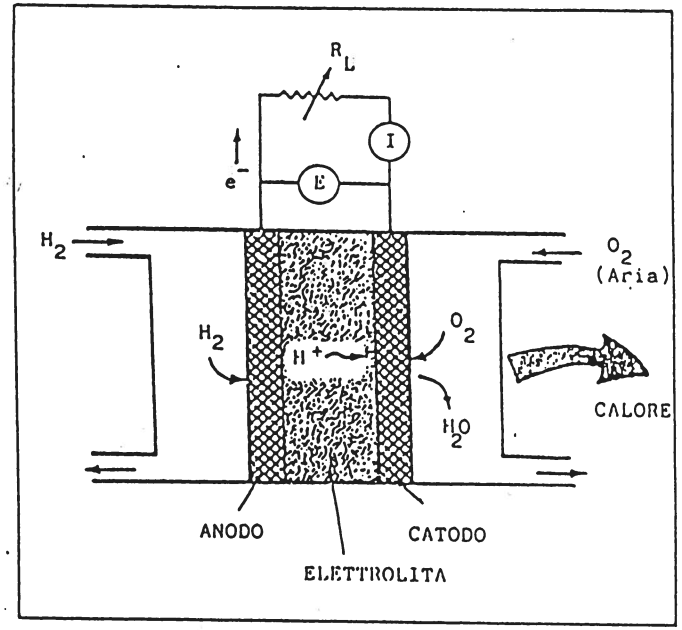

Fig. 1 - Schema di pila a combustibile

A) $H_2 = 2H^+ + 2e^-$

C) $\frac{1}{2}O_2 + 2H^+ + 2e^- = H_2O$

$H_2 + \frac{1}{2}O_2 = H_2O$

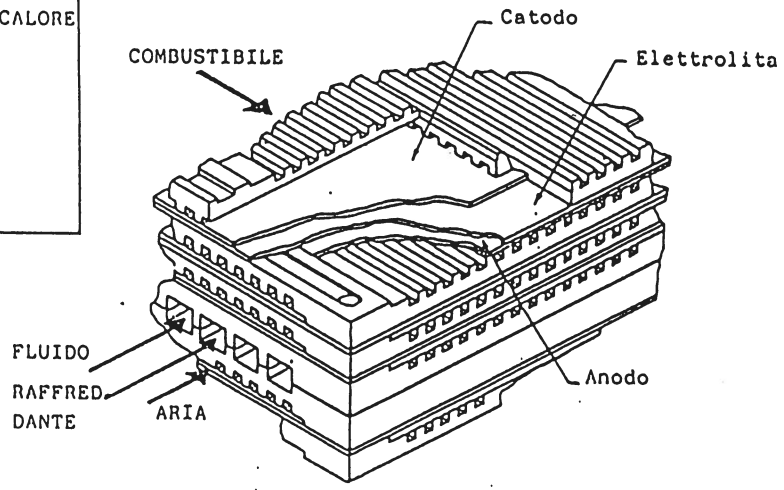

Fig. 2 - Modulo di celle ad H_3PO_4

SLIDE No. 28: B. Leonardis, M. Leonini, from Reference 15.

Table 1 Development target specifications of 50kW class fuel cell stack

Power density	0.2W/cm²
Working pressure	Normal pressure
Average operating temperature	190°C
Effective electrode area	2,000cm² class
Electrode construction	Ribbed substrate
Cooling method	Water cooling

Fig. 1 Structure of fuel cell stack

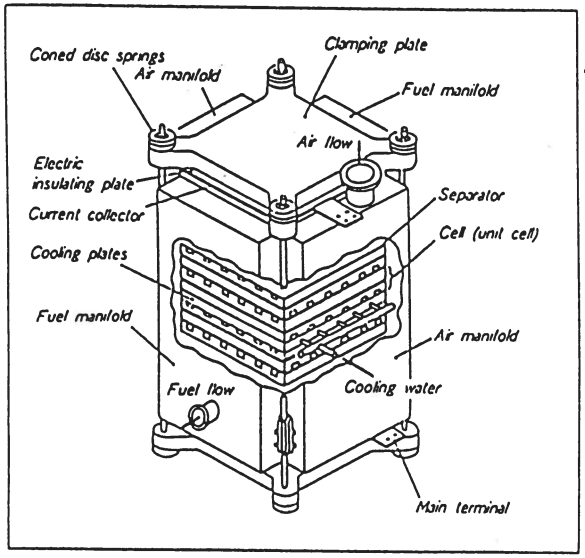

Fig. 1 Structure of phosphoric acid fuel cell electrode

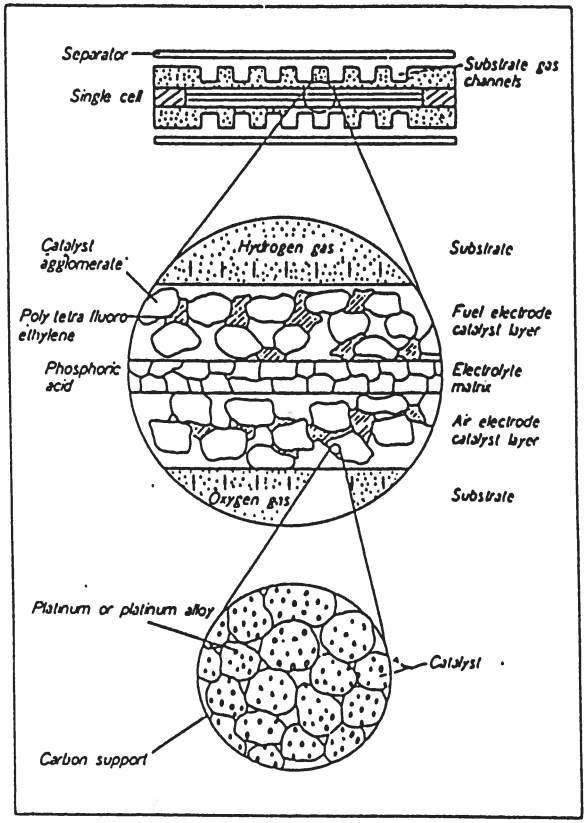

SLIDE No. 29: T. Hirota, N. Nakajima, from Reference 24 (figure on the left).

K. Harashima, H. Enomoto, T. Nakanishi, from Reference 25 (figure on the right).

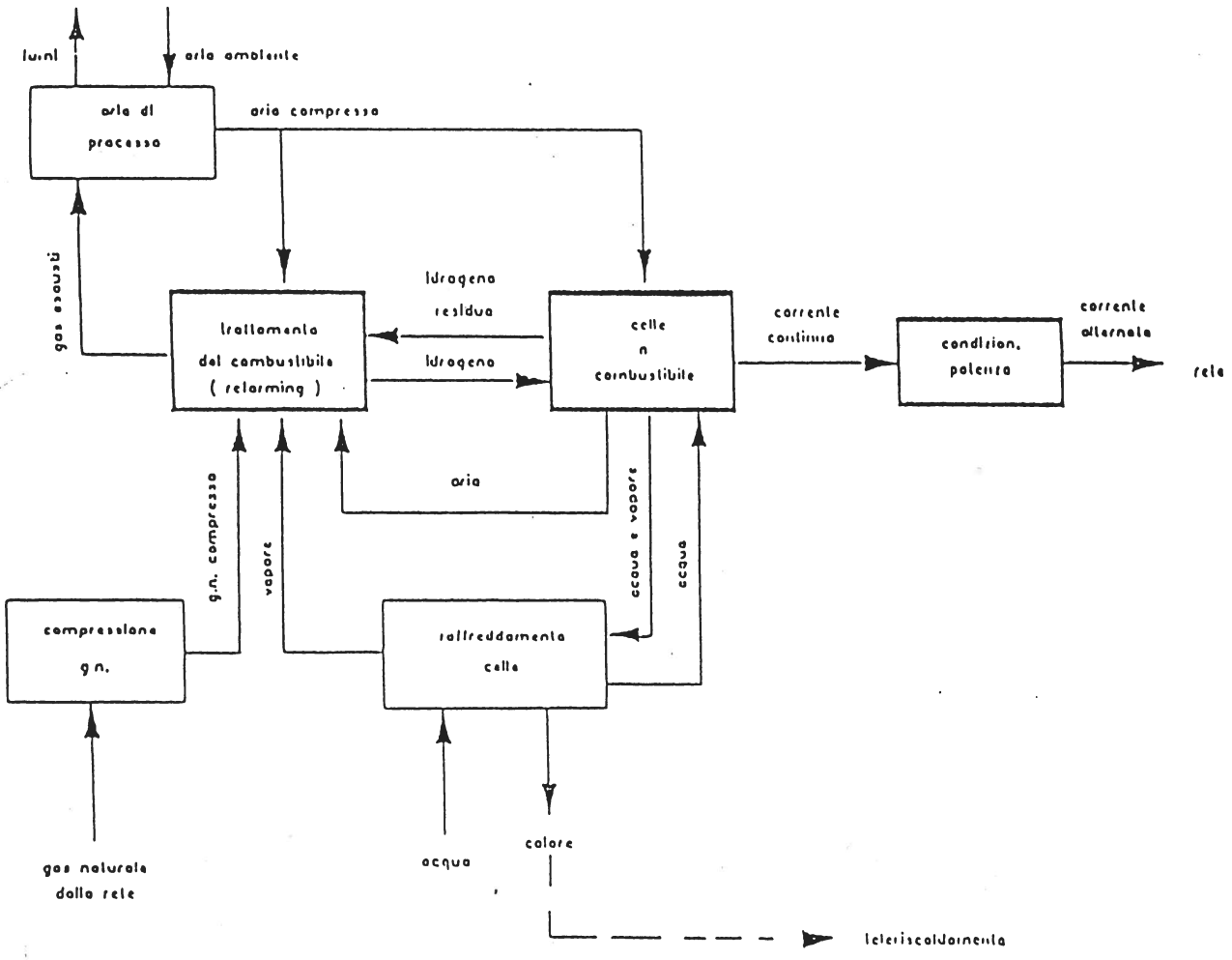

FIG. 1 - Diagrammi a blocchi dei principali sistemi dell'impianto Celle a Combustibile.

SLIDE No.30: A. Dufour, from Reference 22.

- potenza elettrica erogata in circa 50 kW_e;
- peso 8500 kg;
- ingombri 2,6 x 3,2 m, altezza 2,2 m;
- rendimento elettrico 38,5%;
- rendimento totale 80%;
- energia termica disponibile a Tmax = 70 °C;
- calore non utilizzabile (dispersioni) 20%;
- alimentazione con gas di rete;
- necessità di collegamento con la rete elettrica nelle fasi di avviamento e fermata;
- esercizio non in parallelo alla rete con carichi indipendenti resistivi o reali;
- emissioni:
  - SO_x = max 5 mg/Nm³
  - NO_x = max 15 mg/Nm³
  - CO = max 150 mg/Nm³
  - particolato = max 5 mg/Nm³

SNAM ENIRICERCHE MILANO

AEM MILANO

Tabella 1 - Caratteristiche di interfaccia, dati di progetto e prestazioni attese

• Ambiente	temperatura minima	-15°C	• Emissioni	NOx	30 mg/Nm³
	temperatura massima	40°C		SOx	0,6 mg/Nm³
	umidità	fino la 100%		particolato	non rilevabile
• Area occupata	totale edificio	1600 m²	• Rumore	continuo	45 dBA
	area d'impianto	700 m²		sporadico	55 dBA
• Combustibile	tipo	gas naturale	• Caratteristiche elettriche	potenza c.c.	1340 kW
	pressione	1,2 bar		potenza netta a.c.	1180 kW
	P.C.I.	8280 kCal/Nm³		tensione alla rete	23 kV
	Zolfo totale	30 mg/Nm³		frequenza	50 Hz
	Azoto	2,1 % (vol)		armoniche totali	< 5%
• Rendimento elettrico	potenza netta a.c./ P.C.I. gas naturale	40%	• Caratteristiche operative	campo di potenza	30÷100%
				variazione di carico	10%/min
• Calore reso in aerotermo	alta temperatura	840 Mcal/h	• Tempo di avviamento	da freddo	6 ore
	bassa temperatura	280 Mcal/h		da stand-by	10 min

SLIDE No. 31: D. Casati, V. Quinto, from Reference 26 (upper table). V. Cincotti, D. Sardone, M. Sparacino, from Reference 27 (lower table).

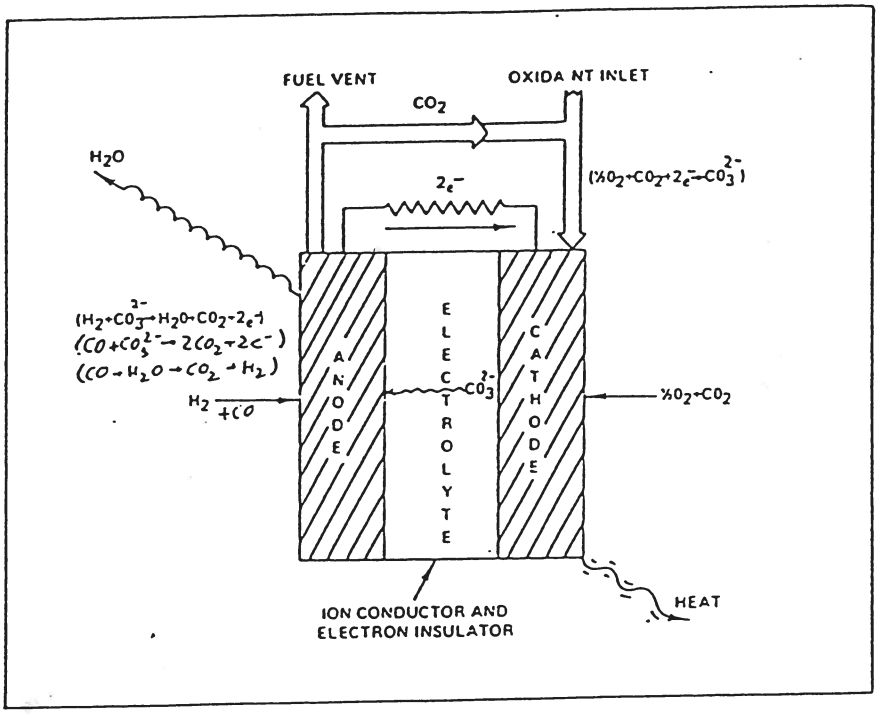

Fig. 1 - Schema di funzionamento di una MCFC (Molten Carbonate Fuel Cell)

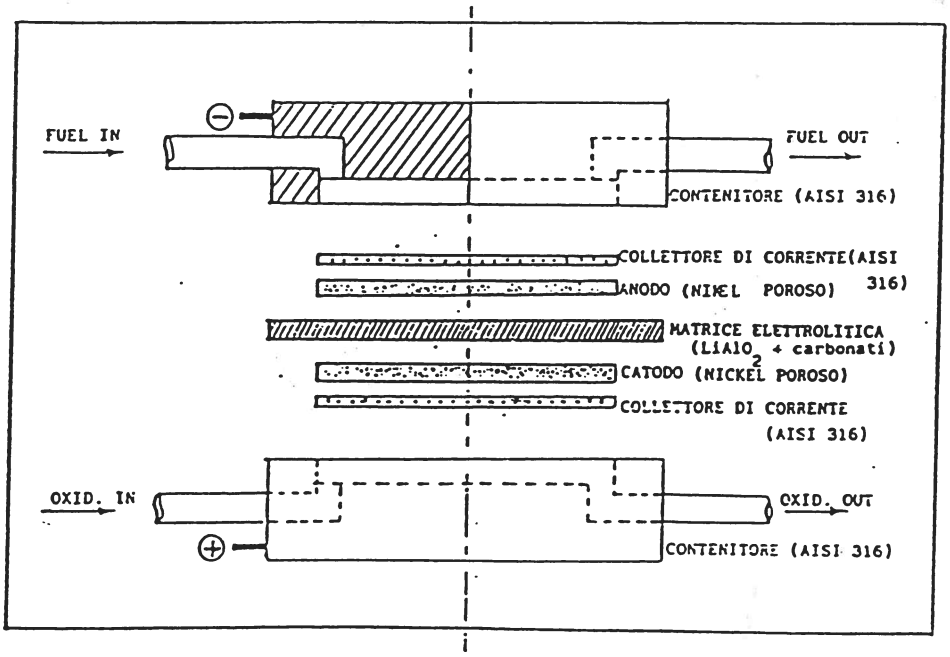

Fig. 2 - Componenti della cella Ansaldo (Molten Carbonate Fuel Cell)

SLIDE No. 32: A. Dufour, F. Galbiati, from Reference 16.

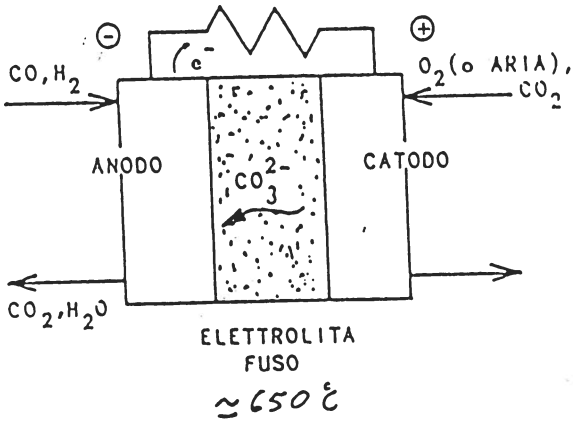

Fig. 2 - Schema di funzionamento di una cella a carbonati fusi.

Le semireazioni anodiche sono:

$CO + CO_3^{2-} \rightarrow 2CO_2 + 2e^-$

$H_2 + CO_3^{2-} \rightarrow H_2O + CO_2 + 2e^-$

La semireazione catodica:

$CO_2 + \frac{1}{2} O_2 + 2e^- \rightarrow CO_3^{2-}$

Le reazioni complessive risultano:

$CO + \frac{1}{2} O_2 \rightarrow CO_2$

$H_2 + \frac{1}{2} O_2 \rightarrow H_2O$

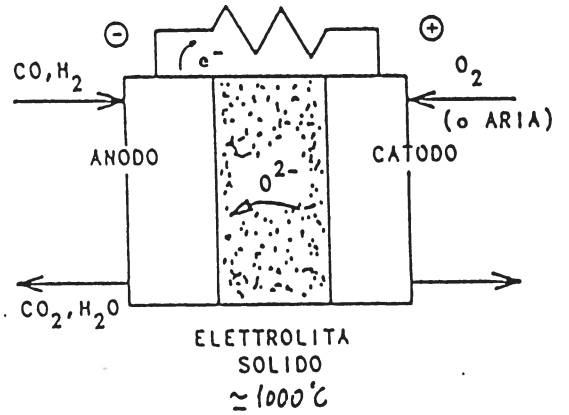

Fig. 1 - Schema di funzionamento di una cella ad ossidi metallici.

Le semireazioni anodiche sono:

$CO + O^{2-} \rightarrow CO_2 + 2e^-$

$H_2 + O^{2-} \rightarrow H_2O + 2e^-$

La semireazione catodica:

$\frac{1}{2} O_2 + 2e^- \rightarrow O^{2-}$

Le reazioni complessive risultano:

$CO + \frac{1}{2} O_2 \rightarrow CO_2$

$H_2 + \frac{1}{2} O_2 \rightarrow H_2O$

SLIDE No. 33: G.Saccenti, R. Tartarelli, C. Zeppi, from Reference 17.

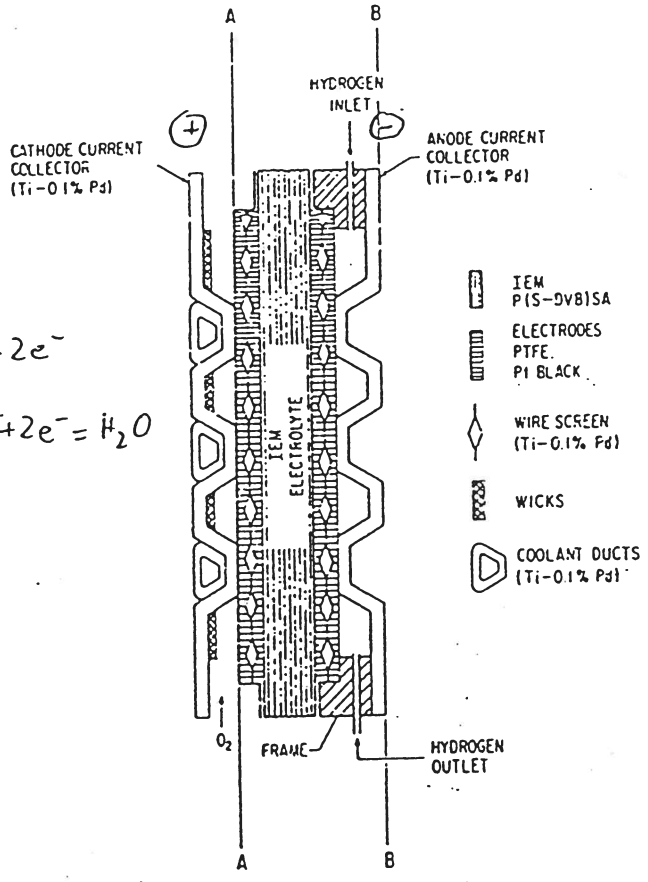

A) $H_2 = 2H^+ + 2e^-$

C) $\frac{1}{2}O_2 + 2H^+ + 2e^- = H_2O$

$\frac{1}{2}O_2 + 2H^+ + 2e^- = H_2O$; $H_2 = 2H^+ + 2e^-$
cathode anode

Fig. 14.11-2 Schematic diagram of a General Electric H_2/O_2 cell for spacecraft.

stacking factor : 6 cell to the inch (0.16" per ale)

SLIDE No. 34: H.A. Liebhafsky, E.J. Cairns, from Reference 1.

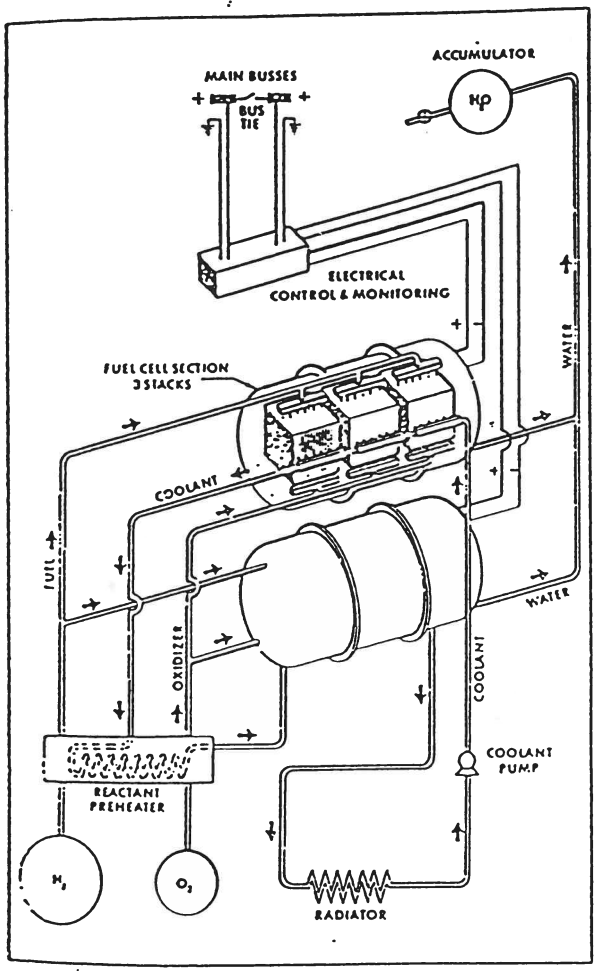

Fig. 14.11-1 Fuel-cell system for Gemini spacecraft [9].

Stack: 32 cells in series (0,78 V/cell),
dimensions 22,5 × 22,5 × 12,5 cm
Battery: 3 stacks in parallel, 40 A, 25 V, 1 kW
37 mA/cm²

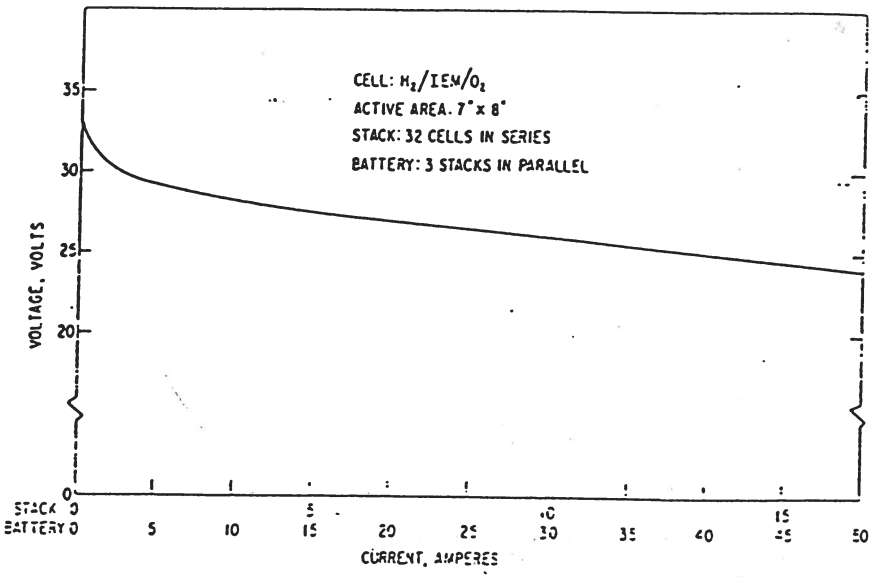

Fig. 14.11-5 Performance curves for stack and battery of Fig. 14.1-1. The lower currents are for the battery.

SLIDE No. 35: H.A. Liebhafsky, E.J. Cairns, from Reference 1.

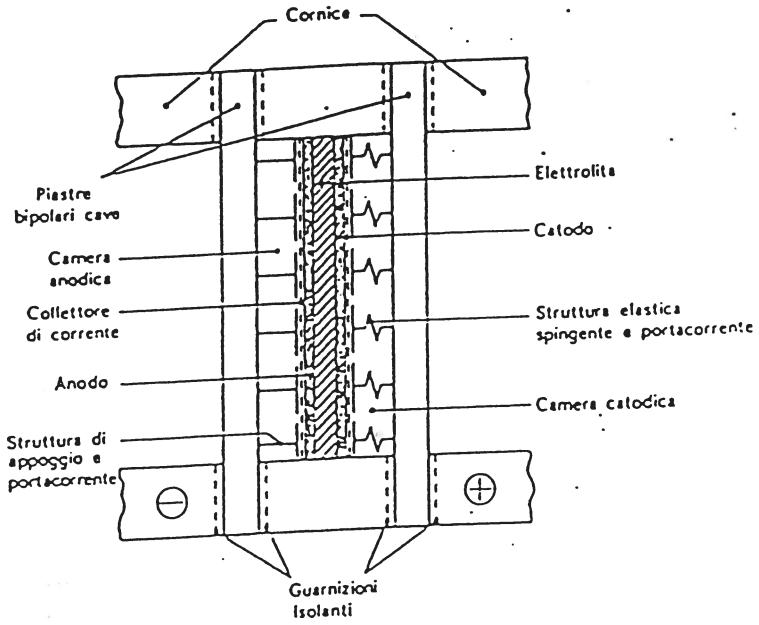

Fig. 6 - Dettaglio di un elemento di uno stack di SPEFC.

DNP stack characteristics

design power	5 kW
voltage	50 V
current	100 A
anodic feeding	hydrogen
cathodic feeding	air
anodic flow rate	2 stech.
cathodic flow rate	2 stech.
gas humidification	stack integrated
operating pressure	3 bar
operating temperature	70 °C
cooling fluid	H2O demi
cooling fluid flow rate	2 m3/h
stack weigth	130 kg
stack dimensions	1100 mm L
	300 mm H
	300 mm W
power density (present - 1993)	0.038 kW/kg
	0.050 kW/l
power density (expected - 1995)	0.063 kW/kg
	0.062 kW/l

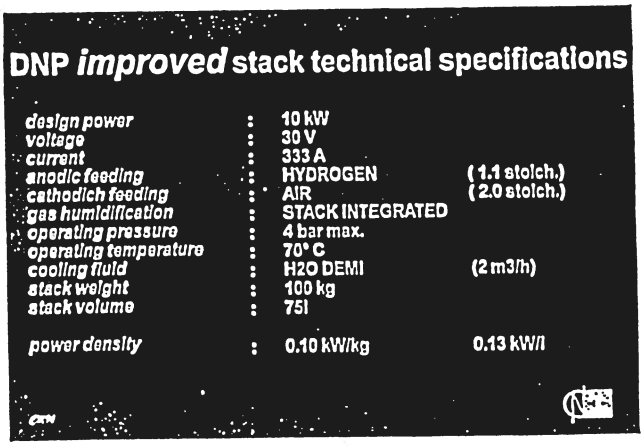

SLIDE No. 36: G. Bianchi, from Reference 29 (figure).
C. Mantegazza, B. Marcenaro, from Reference 35 (tables).

Bus Characteristics

Configuration	12 m	Fuel cell type	PEM
Max.speed	60 km/h	Fuel consumption	15 kg LH2 per 100 km
Max. slope	16%	Fuel cell power	35 kW
Passenger capacity	100	Traction system	600 VAC electric drive
Operating range	300 km	Traction power	120 kW nominal
Fuel	Liquid H2	Buffer battery	Pb-Acid 600V - 100 Ah

Block Diagram

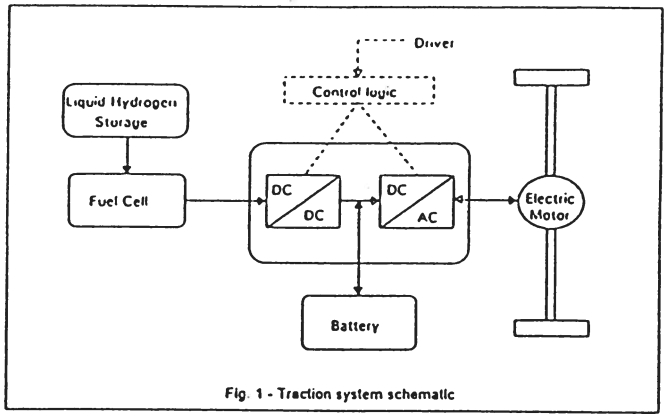

Fig. 1 - Traction system schematic

EQHHPP - bus layout

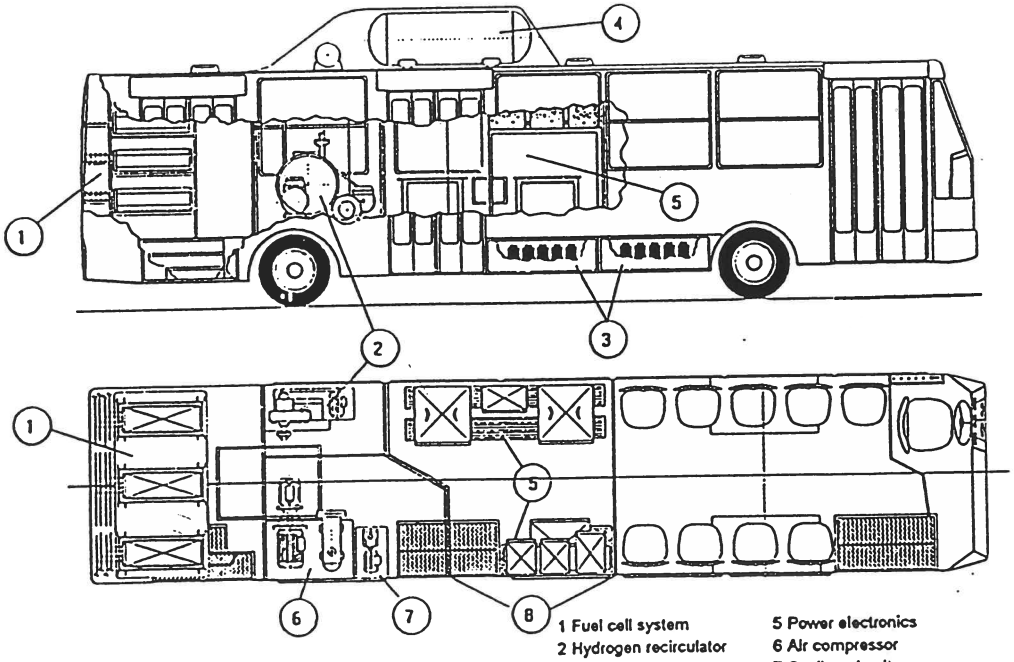

1 Fuel cell system
2 Hydrogen recirculator
3 Battery
4 Liquid hydrogen storage
5 Power electronics
6 Air compressor
7 Cooling circuit pump
8 Safety walls

ANSALDO
Ricerche

SLIDE No. 37: C. Mantegazza, B. Marcenaro, from Reference 35.

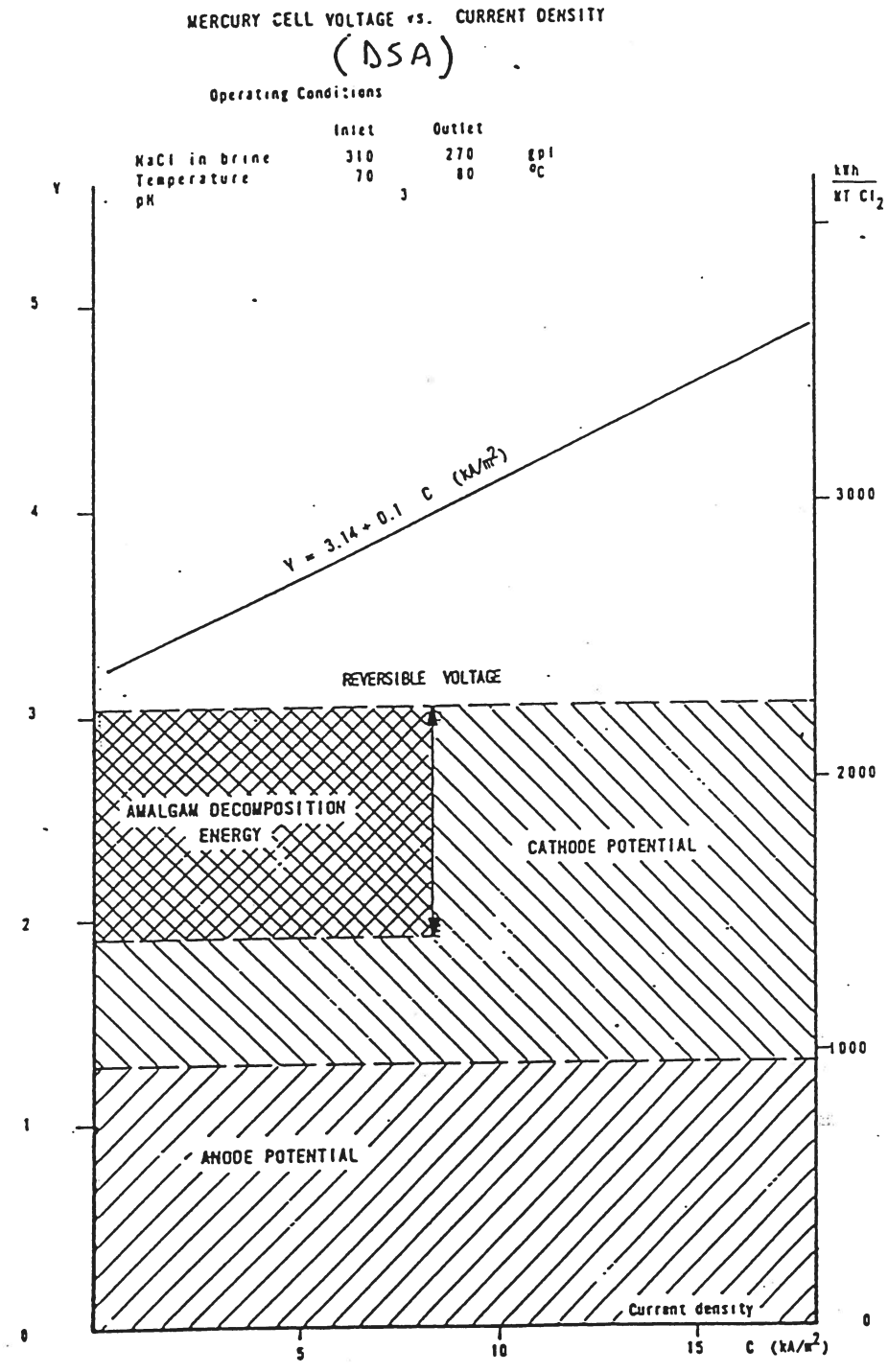

SLÍDE No. 38: by courtesy of De Nora Permelec S.p.A.

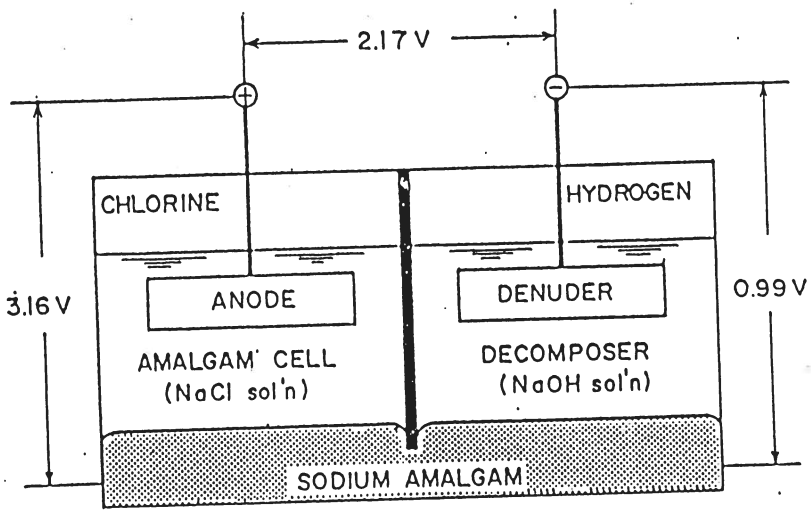

FIGURE 4.18. Combination of the amalgam cell and the amalgam decomposition cell.

Amalgam cell, decomposition voltage $E_d(M) = 3.16$ V

Amalgam decomposition, electromotive force $E_f = 0.99$ V

Diaphragm cell, decomposition voltage $E_d(D) = 2.17$ V

$$E_d(M) - E_f = E_d(D)$$

SLIDE No. 39: F. Hine, from Reference 10.

schema elettrico:

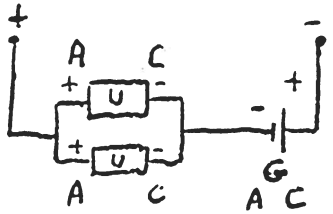

U = utilizzatore
G = generatore
A = anodo
C = catodo

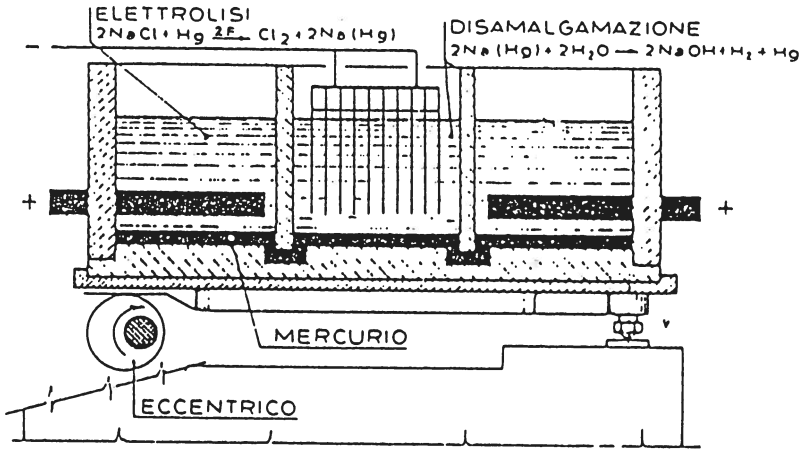

Fig. X.1 -- Cella oscillante di Castner: schema originale [1].

(1892 - 1894)

SLIDE No. 40: P. Gallone, from Reference 2.

Table 4. Recovery of electricity with an amalgam denuder using an air cathode

1. Sodium amalgam - Cl_2 generating cell

   (DSA) Cl_2 | NaCl(30%) | Na(Hg)-liq.

   Reaction: $2\ NaCl + (Hg) \longrightarrow 2\ Na\ (Hg) + Cl_2$

   E(rev) = 3.3 V
   E(actual) = 3.8 ÷ 4.5 V

2. O_2 (air) cathode-sodium amalgam denuder cell

   O_2 (air) | NaOH(50%) | Na(Hg)

   Reaction: $4\ Na(Hg) + O_2 + 2\ H_2O \longrightarrow 4\ NaOH + (Hg)$ $\begin{cases} 4Na(Hg) = 4Na^+ + 4e^- \\ 2H_2O + O_2 + 4e^- = 4OH^- \end{cases}$

   E(rev) = 2.4 V
   E(actual) = ∿ 1.5 V

3. Overall reaction for cells 1 and 2

   $4\ NaCl + O_2 + 2\ H_2O \longrightarrow 4\ NaOH + 2\ Cl_2$

   E(net,rev) = 0.9 V
   E(net,actual) = 2.3 ÷ 3.0 V
   Electricity saving: 33 to 40%

SLIDE No. 41: E. Yeager, from Reference 5.

THEORETICAL ENERGY SAVING WITH AN OXYGEN CATHODE AND ACTUAL VOLTAGE OBTAINED

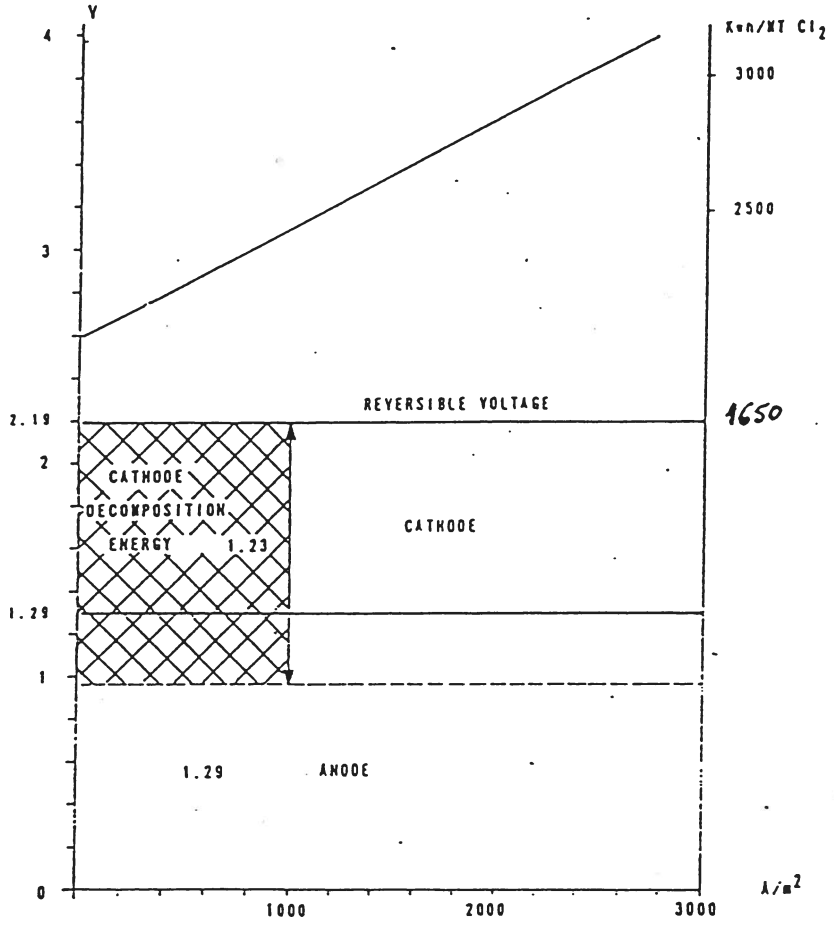

SLIDE No. 42: by courtesy of De Nora Permelec S.p.A.

Table 4. Recovery of electricity with an amalgam denuder using an air cathode

1. Sodium amalgam - Cl_2 generating cell

   (DSA) Cl_2 | NaCl(30%) | Na(Hg)-liq.

   Reaction: $2\ NaCl + (Hg) \longrightarrow 2\ Na\ (Hg) + Cl_2$

   E(rev) = 3.3 V
   E(actual) = 3.8 ÷ 4.5 V

2. O_2 (air) cathode-sodium amalgam denuder cell

   O_2 (air) | NaOH(50%) | Na(Hg)

   Reaction: $4\ Na(Hg) + O_2 + 2\ H_2O \longrightarrow 4\ NaOH + (Hg)$ $\begin{cases} 4Na(Hg) = 4Na^+ + 4e^- \\ 2H_2O + O_2 + 4e^- = 4OH^- \end{cases}$

   E(rev) = 2.4 V
   E(actual) = ∿ 1.5 V

3. Overall reaction for cells 1 and 2

   $4\ NaCl + O_2 + 2\ H_2O \longrightarrow 4\ NaOH + 2\ Cl_2$

   E(net,rev) = 0.9 V
   E(net,actual) = 2.3 ÷ 3.0 V
   Electricity saving: 33 to 40%

SLIDE No. 41: E. Yeager, from Reference 5.

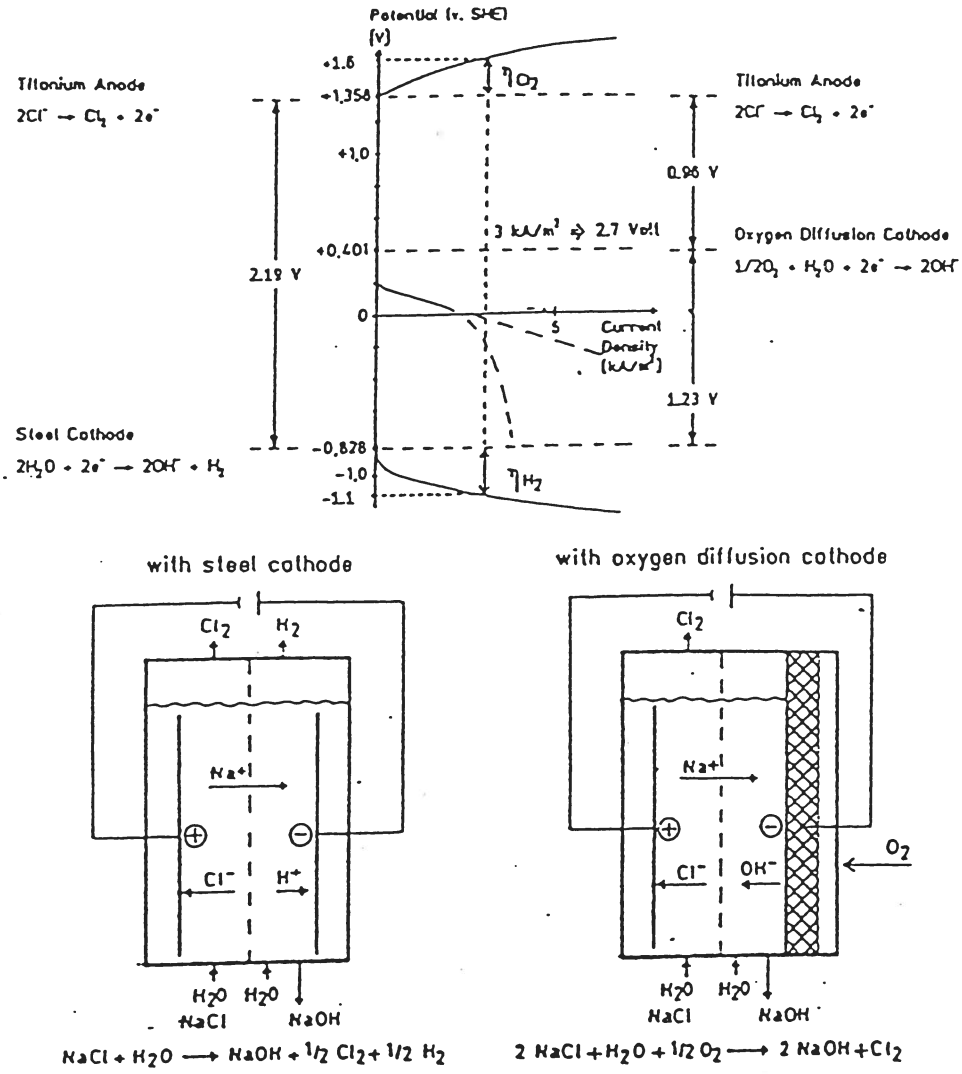

Figure 11. Electrode Potentials in Membrane Processes

SLIDE No. 43: K.H. Simmrock, from Reference 8.

Table. 2 Chlor-alkali applications for O_2 cathodes in conjunction with membrane cells

1. H_2 generating membrane cell

(DSA) Cl_2 | NaCl (15%) ¦ NaOH (30%) | H_2 (Fe, cat.) (85°C)

Reaction: $2\ NaCl + 2\ H_2O \longrightarrow 2\ NaOH + Cl_2 + H_2$

E(Rev) = 2.2 V
E (Actual) = 3.6 V

2. O_2 (air) consuming membrane cell

(DSA) Cl_2 | NaCl (15%) ¦ NaOH (30%) | air (cat.) (85°C)

Reaction: $2\ NaCl + 1/2\ O_2 + H_2O \longrightarrow 2\ NaOH + Cl_2$

E(Rev) = 1.0 V
E(Actual) = 2.5 V

3. Recovery of electrical energy from H_2 with H_2-air fuel cell

(DSA) Cl_2 | NaCl (15%) | NaOH (30%) | H_2 (Fe, cat.) (85°C)
H_2 (cat.) | H_3PO_4 | air (cat.) (190°C)

Overall reaction: $2\ NaCl + 1/2\ O_2 + H_2O \longrightarrow 2\ NaOH + Cl_2$

E(fuel cell-actual)* = ∿ 0.7 V
E(net) = E (chlor-alkali)-E (fuel cell) = ∿ 2.9 V

*Assuming phosphoric acid fuel cell operating at ∿ 190°C with cogeneration of heat for evaporation to concentrated caustic.

SLIDE No. 44: E. Yeager, from Reference 5.

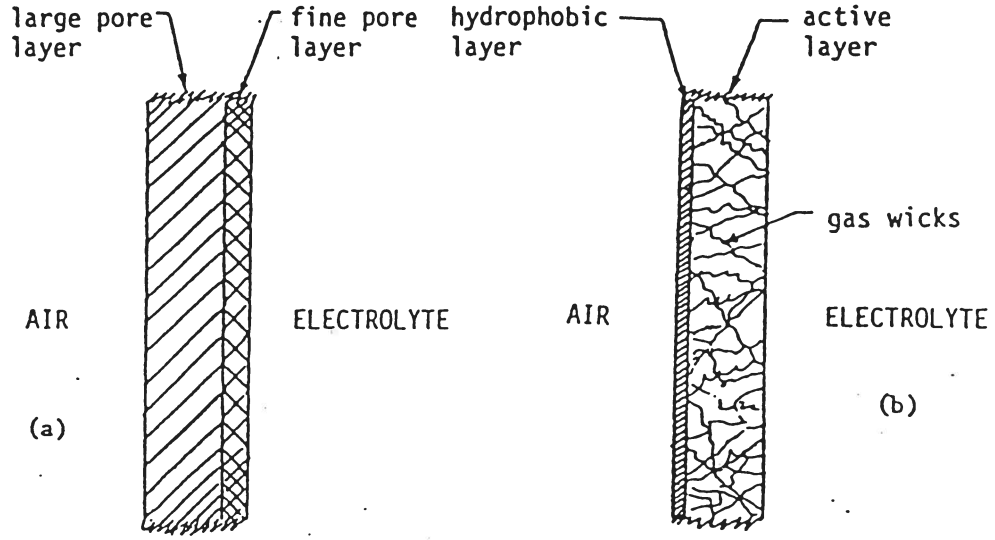

Figure 2a. O_2 cathode structure: hydrophilic type (not scaled).
2b. Semi-hydrophobic type (not scaled).

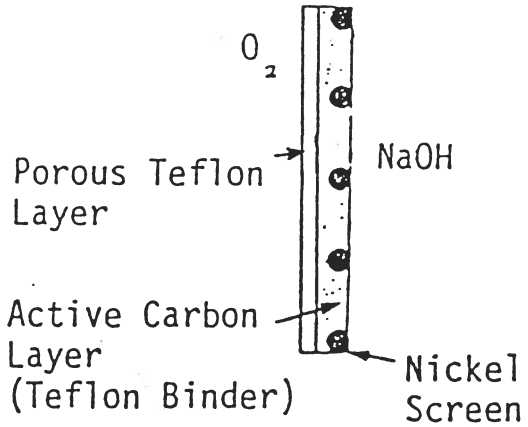

Figure 3. Semihydrophobic electrode structure.

SLIDE No. 45: E. Yeager, from Reference 5.

CAUSTIC SODA PRODUCTION PLANT WITHOUT GENERATION OF CHLORINE USING SODIUM CARBONATE / BICARBONATE AS RAW MATERIAL

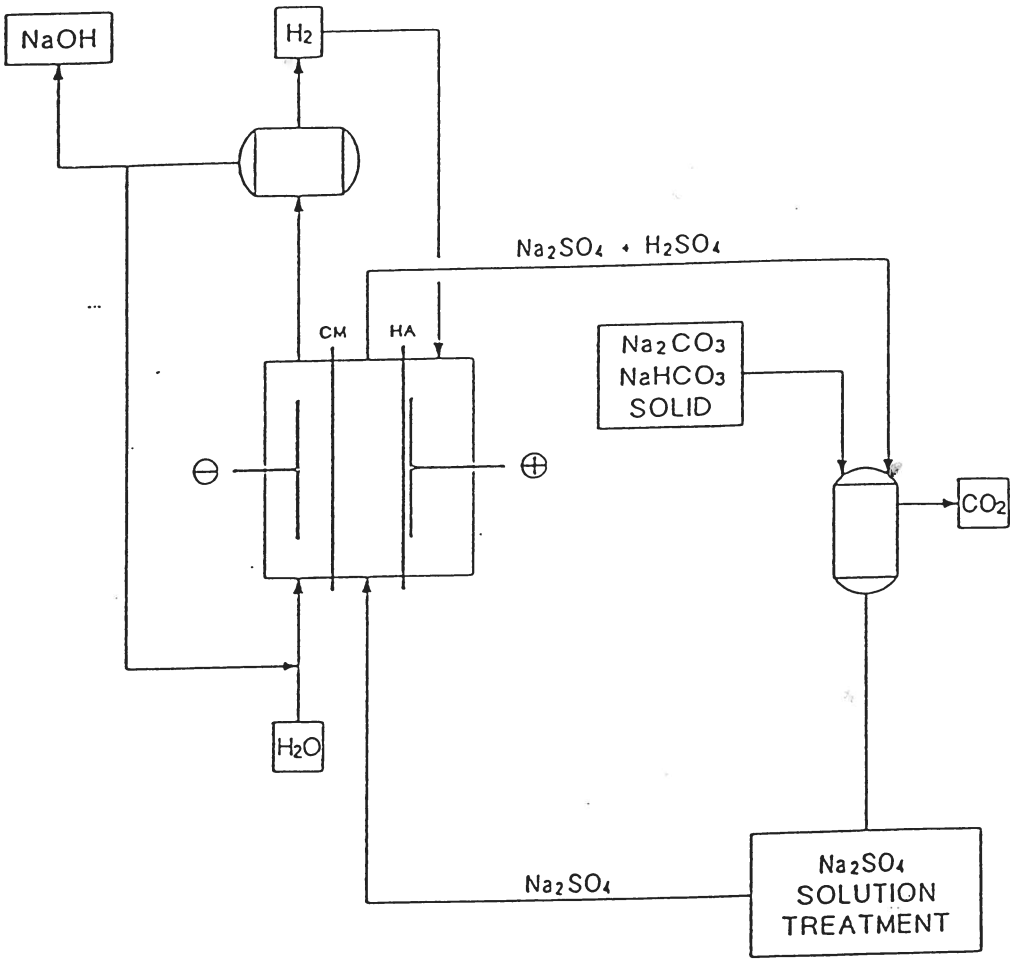

CM : Cation-Exchange Membrane
HA : Hydrogen Depolarized Anode

$$Na_2CO_3 + H_2O + kWh \longrightarrow 2\ NaOH + CO_2$$

Titanor Components Ltd - De Nora Group - Technical Seminar, Goa (India), February 22, 1992

SLIDE No. 46: G. Faita, from Reference 12.

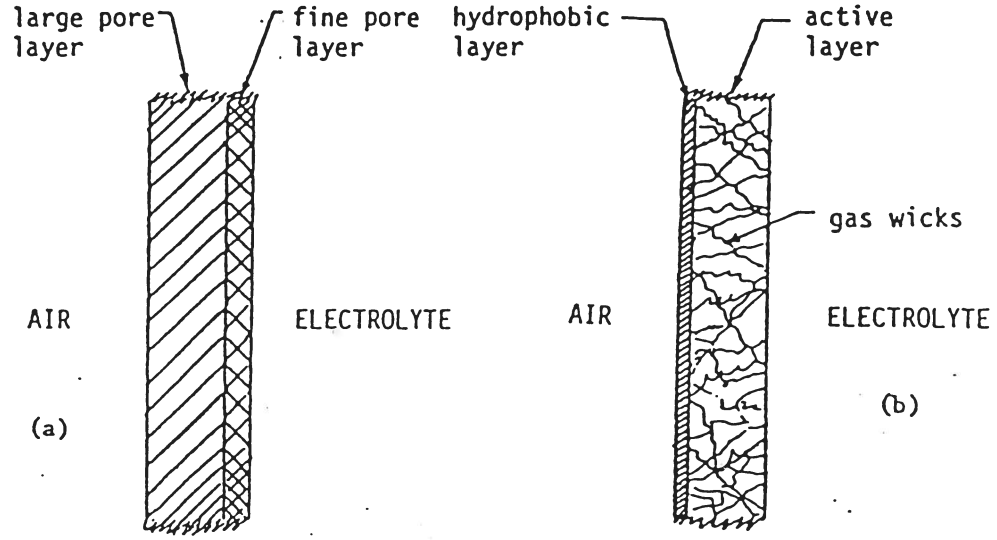

Figure 2a. O_2 cathode structure: hydrophilic type (not scaled).
2b. Semi-hydrophobic type (not scaled).

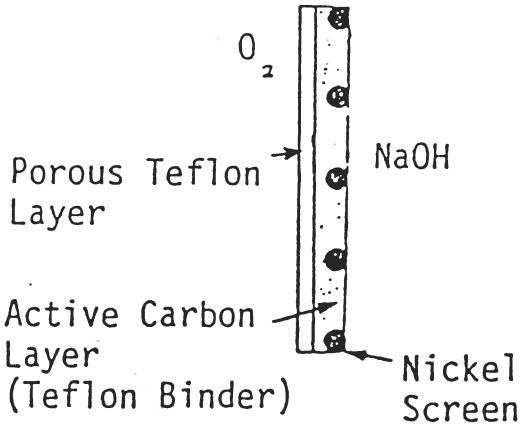

Figure 3. Semihydrophobic electrode structure.

SLIDE No. 45: E. Yeager, from Reference 5.

NEUTRAL SALTS SPLITTING BY ELECTROLYSIS WITH RECOVERY OF CAUSTIC SODA AND ACID

CM : Cation-Exchange Membrane
AM : Anion-Exchange Membrane
HA : Hydrogen Depolarized Anode

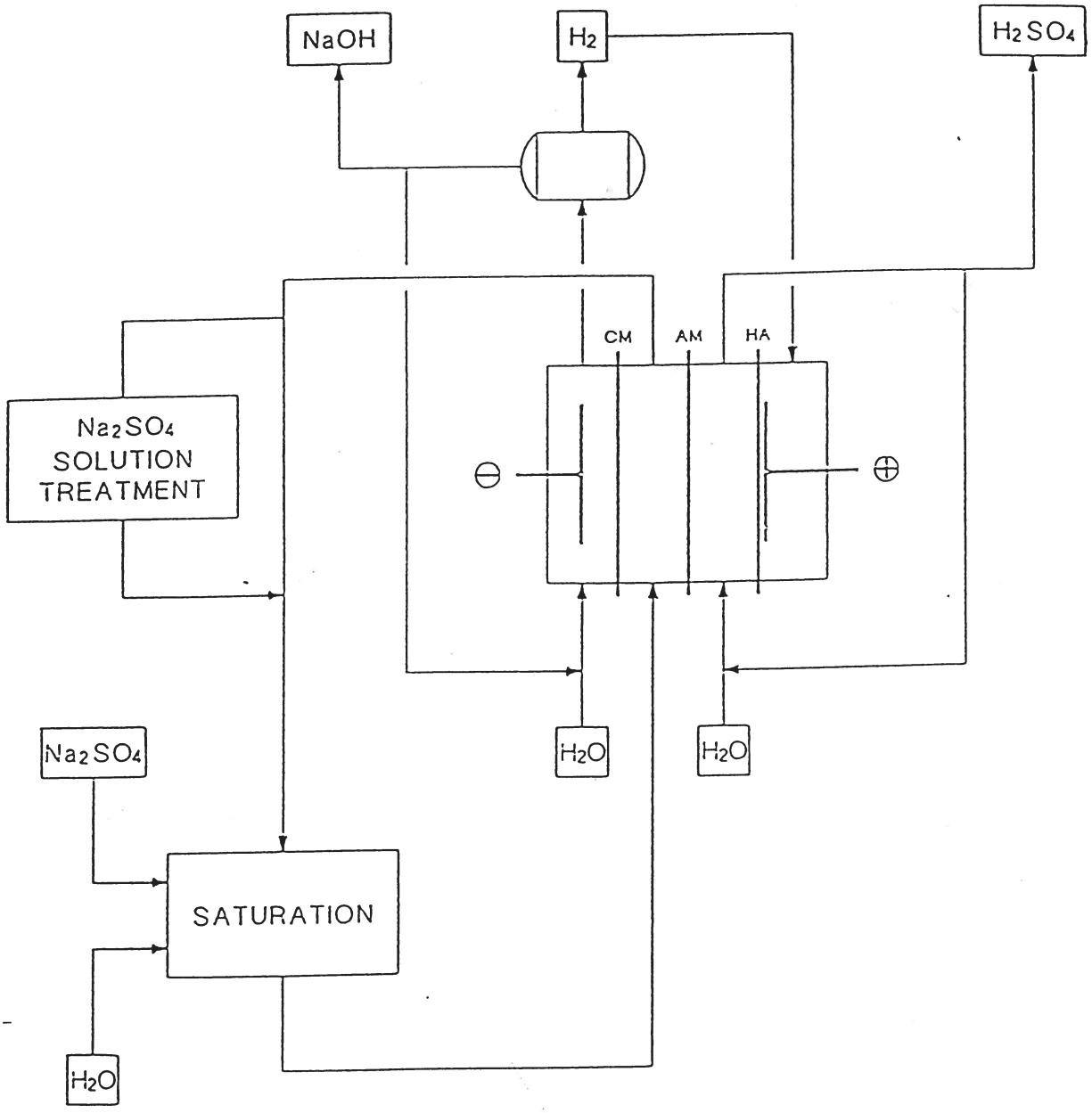

Titanor Components Ltd - De Nora Group - Technical Seminar, Goa (India), February 22, 1992

SLIDE No. 47: G. Faita, from Reference 12.

SCHEMATIZATION OF THE INTERNAL STRUCTURE OF A CONVENTIONAL GAS DIFFUSION ELECTRODE

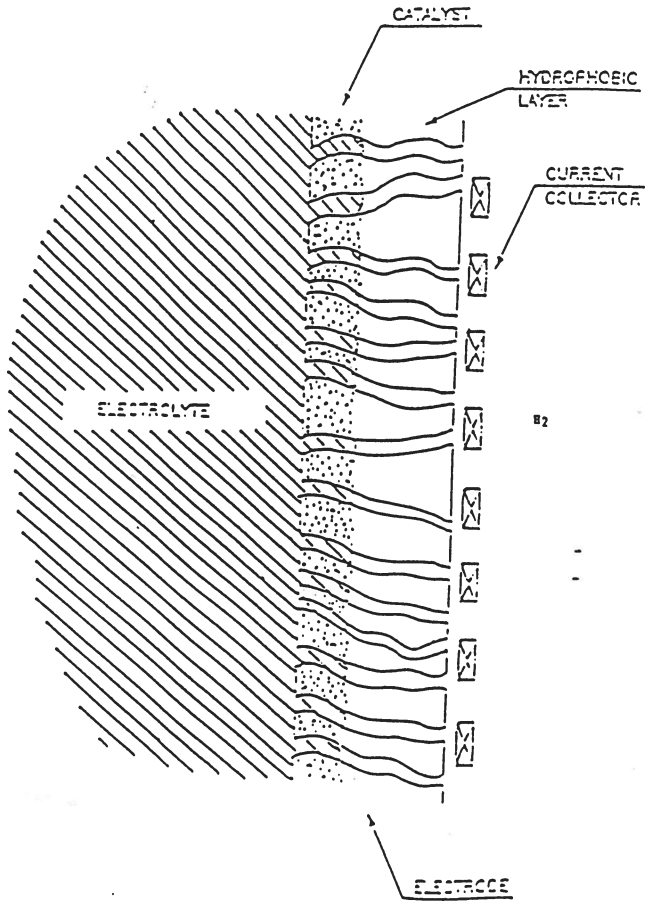

SCHEMATIZATION OF A GAS DIFFUSION ELECTRODE COMPRISING A CATION EXCHANGE MEMBRANE

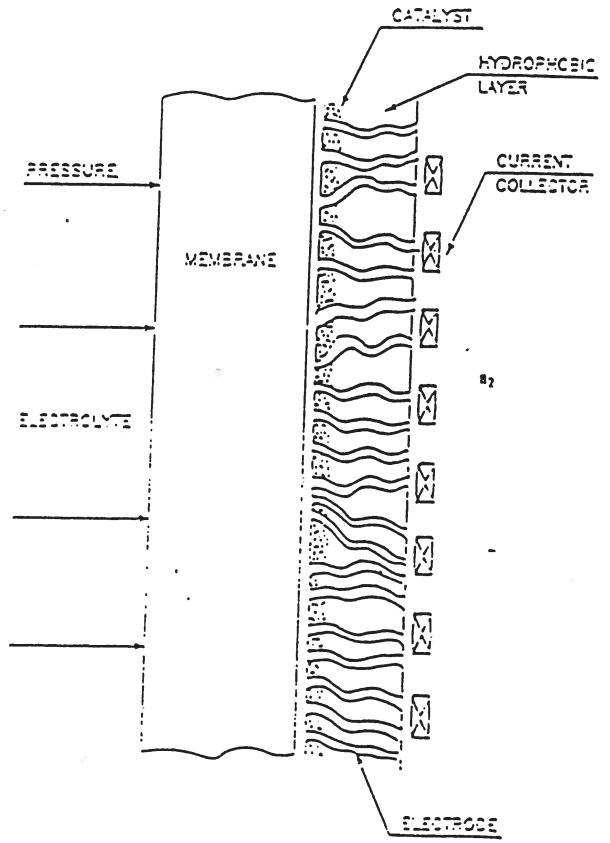

SLIDE No. 48: G. Faita, from Reference 32.